# Spatial Watershed Iterative Loading (SWIL) 5.0 Model Update and Future Land Use Impact

CLAUDIA LISTOPAD, PH.D., GISP

Prepared For:

Prepared By:

# Table of Contents

# Background and Purpose of the Model

FDEP has identified the Indian River Lagoon (IRL) and Banana River Lagoon (BRL) as impaired waterbodies due to nutrient over-enrichment. In March 2009, FDEP issued total maximum daily loads (TMDLs) for the IRL and BRL requiring reductions of total nitrogen (TN) and total phosphorus (TP) in stormwater runoff by 21% to 69% across the Lagoon (Gao, 2009). The TMDL was established on the basis of a relationship between nutrient loading and seagrass depth limits. Nutrient loading estimates were calculated using the Pollution Load Screening Model (PLSM), originally developed for smaller areas within the IRL (Bergman and Donnangelo, 1995, 1996a, 1996b, 1998), and later expanded to the entire IRL drainage by SJRWMD to represent loads for the year 2000 (Adkins *et al*., 2004). Seagrass depth limits were developed by SJRWMD from a 1943 to 2001 series of photo-interpreted seagrass coverages.

Through an Interlocal Agreement and a Joint Participation Agreement, all MS4 permittees within the Brevard County portion of the IRL (17 entities) partnered to fund a Study Team to update and refine the 2000 PLSM model and associated TMDLs for the IRL. After the TMDL was established, additional data were collected, enabling the Study Team to re-visit the TMDL and address pertinent questions that have arisen regarding pollutant loading and seagrass relationships. The Spatial Watershed Iterative Loading (SWIL) model was developed as part of this study to incorporate more available data, more recent conditions, and more temporally fine datasets. SWIL is a custom ESRI ArcGIS toolset, originally designed to provide a continuous monthly simulation of runoff (surface and baseflows) over a 16-year period, yielding a more robust representation of pollutant loadings and freshwater volumes in the IRL.

The goal of SWIL is to provide a GIS-based model that can be adaptive to changes in input and can batch complex processes through several months or years on demand. SWIL aims to provide both spatially and temporally fine-scale volumes and loads (TP and TN), allowing input data to be related to water quality parameters. Since temporal and spatial differences in water quality appear essential in understanding the Indian River Lagoon and Banana River Lagoon system, an input watershed model that provides data at the same fine scales is critical to the TMDL process. The portability of the model (a toolset within ArcGIS) and flexibility of its design are key features of the SWIL.

The SWIL model has been updated since the initial version was developed in 2012 (SWIL 1.0). By July 2014, SWIL 2.0 was released focusing on addressing initial FDEP comments, improving the ease of execution, and reducing the overall processing time. SWIL 3.0, released in April 2015, focused on improving model calibration to the measured available gage data, which included a change in the methodology to derive baseflow volumes and loads. SWIL 3.0 also incorporated the newly released evapotranspiration (ET) raster datasets, which were updated using the newly improved Mu *et al.*'s ET algorithm (2011). SWIL 4.0 was developed in support of the 3D Numerical Modeling effort for the Indian River Lagoon and Banana River led by Florida Institute of Technology. This version required three major changes: 1) expansion of the model extent to provide nutrient loadings from Ponce Inlet to Fort Pierce 2) temporal expansion from 2011 through August 2015, and 3) converting the model from two to three land use/treatment time steps. As each land use type is associated with a specific runoff coefficient, the latter step of incorporating an additional time step of land use and treatments in the model run period provides a better method to capture changes in urbanization over time, critical with model runs that span two decades or more. As the watershed becomes more urbanized, imcreases in impervious area typically drive increases in direct runoff volumes and associated loads. Being able to capture when these land use alterations occurred and apply them to the most appropriate modeling time period increases the accuracy of model predicted volumes and nutrients.

The most recent SWIL update, version 5.0, included two major changes: 1) the expansion of the model boundary to include the St. Lucie Estuary watershed and 2) temporal expansion of the model to include volume and loading predictions through December 2017. The main objective of the model development was to produce monthly estimated TN and TP loads from January 1995- through December 2017 for 87 subsegments of the Lagoon watershed, so these could be integrated in Florida Tech's 3D numeric nutrient model.

The project task also included integrating a previously AEI-developed model for the United States Air Force (USAF, 45$^{th}$ Space Wing) into the SWIL 5.0 model. The USAF model was specifically developed for the Cape Canaveral Air Force Station (CCAFS) and Patrick Air Force Base (PAFB) as part of their Environmental Compliance Program. This site-specific model reflects a variety of updated inputs datasets, many of which are based on field validation and years of onsite TMDL monitoring efforts. These higher resolution and field calibrated nutrient loads from both military bases were integrated into the Banana River watershed loading model.

Finally, the project task in Year 3 examined the potential impact of future land use of the North Indian River Lagoon (NIRL) watershed on the nutrient loading to the NIRL. Future land use for this watershed was based on Brevard County's and other available municipalities future land use mapping and zoning designations, when available. Increases in watershed urbanization can have the potential to increase runoff volumes and associated nutrient loading to nearby waterbodies. Future scenario modeling efforts are important tools for the development of a watershed-wide resiliency plan.

# Methodology

## SWIL 5.0 Model Development

SWIL 5.0. development required changes in both model processing as well as input data. Most of the processing changes were minor and were required to allow expansion of the model spatial extent. The most critical changes are directly related to modifications in data input, described in the sections below.

The previous model boundary was extended to include a larger watershed area. Previously only the North Indian River Lagoon, the Banana River, and the Central Indian River Lagoon (~11 km into St. Lucie County) were included in the modeling extent. The model boundary for the SWIL 5.0 model was increased to include the St. Lucie Estuary watershed within the TMDL boundary. This was an overall increase of 17 basins across three counties (St. Lucie, Martin, and Okeechobee). Eight basins are located in the South IRL watershed (C-44, BASIN_4, BASIN_5, BASIN_6, MIDDLE_STLUCIE_ESTUARY, SOUTH_COASTAL, SOUTH_FORK, and SOUTH_MID-ESTUARY) and nine basins are situated in the St. Lucie watershed (C-23, C-24, C-25_CONVEYANCE_CANAL, LOWER_STLUCIE_ESTUARY, MID_COASTAL_N, MID_COASTAL_S, NORTH_MID-ESTUARY, STLUCIENORTHFORK, and the UPPERSTLUCIE_ESTUARY). The SWIL 4.0 model boundary was 768,111.76 acres and the SWIL 5.0 model is 1,343,256.14 acres, which is an overall increase of 575,146 acres or a 74.9 % increase in area. Figure 1 shows the spatial increase of the model boundary.

## Land Use Land Cover

This methodology allowed the best source data to be used for capturing land use changes for these three time periods (2000, 2004, and 2015), producing a dataset that covers a large areal extent without gaps, a requirement to run the SWIL model. No aerial photointerpretation or ground validation was performed on the land use layers used in the SWIL model due to both budget and time constraints for such a large watershed. Minor discrepancies in land use interpretation have been previously detected when performing photointerpretation of smaller modeled basins, so greater accuracy in the model could be obtained with an extensive photointerpretative effort.

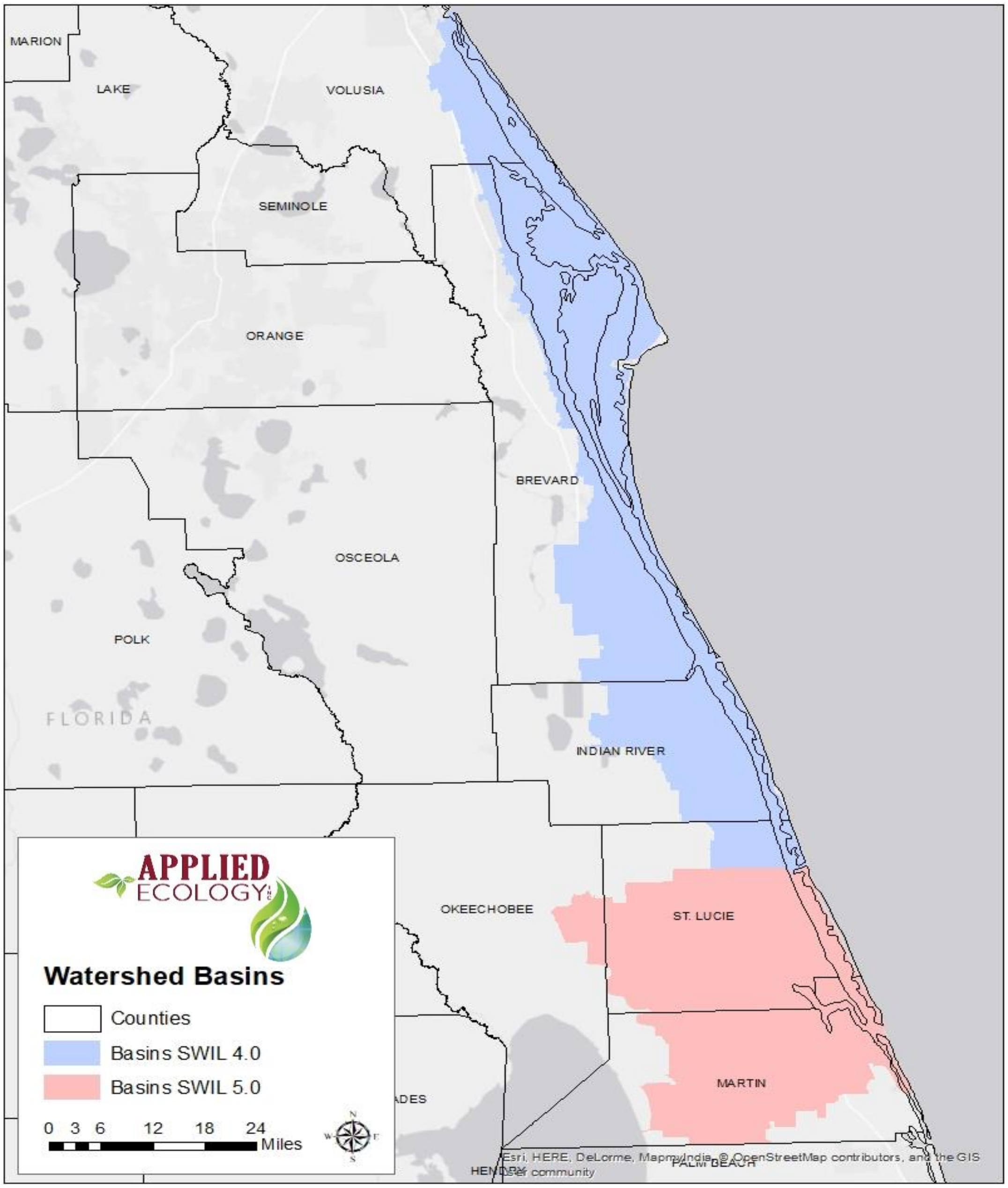


**Figure 1. Model boundary increase from SWIL 4.0 to SWIL 5.0.**

## Treatments

Developed land with stormwater treatment systems has cleaner water leaving the site than developed land with no treatment system. Private subdivisions and commercial properties constructed after 1986 were required by the SJRWMD to treat their stormwater runoff as a condition of their ERP permit. In addition, Brevard County adopted stormwater treatment requirements and began permit review in 1978. For the SWIL model, a treatment layer with higher spatial accuracy and additional information (treatment type) was developed based on Property Appraiser datasets. A subdivision layer was created for residential properties; a year was assigned to each subdivision using the year in which the first house of each subdivision was constructed. We assumed that an approved site plan with constructed stormwater treatment must be in place by no later than the year that the first house was built within the permitted subdivision, and private residential subdivisions built after 1986 (1986-2000 for the 2000 treatment layer, 1986-2004 for the 2004 treatment layer, and 1986-2015 for the 2015 treatment layer) were considered treated. For non-residential individual parcels (commercial or industrial land uses) constructed after 1986, the year of construction was used to capture additional private development treatment data. All treatments delineated in AEI´s layers were assigned a type, either wet detention or dry retention ponds. Treated areas were applied reductions in estimated volumes and nutrient loadings by type, based on Dr. Harper's previously developed work (Harper and Baker, 2007; Harper and Baker, 2015). Treatments for the expanded areas across St. Lucie, Okeechobee, and Martin counties for all required model years (2000, 2004, and 2015) were combined with the previous treatment layers, to form the updated SWIL 5.0 model treatment layers.

## Soils

For every soil type classification, there is an associated infiltration characteristic called the hydrologic soil group (HSG) that is a key component in determining appropriate runoff coefficients "C". Runoff coefficients are critical variables for the development of an accurate watershed loading model. The spatial expansion of the soil hydrologic dataset was an essential preparatory step in order to generate runoff volumes in the SWIL model. Data were obtained from the NRCS (formerly the U.S. Soil Conservation Service) for areas not previously included in the SWIL 4.0 model (Martin, Okeechobee, and the portions of St. Lucie County). Consistent with the previous model, spatial interpolation was used to fill in missing HSG classifications. Some soil types received a dual HSG classification ("A/D", "B/D", or "C/D") where the first letter is indicative of drained or disturbed soils and the second is indicative of undrained or undisturbed soils. Upon further investigation, the appropriate HSG was assigned through the combination of aerial imagery photointerpretation and FLUCCS codes provided by the water management districts. When the majority of a specific soil polygon resided within a FLUCCS code boundary indicative of disturbed or "non-natural condition" soil (e.g., residential, agriculture, commercial, etc.), it was classified as the better-drained soil classification, often "A" or "B" soil types. In contrast to this, when a soil polygon with dual classification appears to be natural (e.g., wetlands, forests, etc.), it was classified as the most poorly drained of the two classifications, typically a "D" code. This designation was only used when assigning missing HSG classification values to the soil datasets. When the FLUCCS code did not correspond with the latest aerial imagery, each soil area was photointerpreted to ensure the application of the correct classification. For example, wetland areas typically received a poorly drained soil classification based upon FLUCCS code as they are natural areas; however, some of these wetlands were altered enough through ditching and urban encroachment that the soil was assigned a more drained classification type.

## Rainfall

The large focus of the watershed model update has been on expanding the input rainfall rasters both spatially and temporally. Rainfall isopleths are developed for each month of the model period, based on rainfall stations with available and adequate data. For more details on methodology, please review Environmental Research and Design, Inc.'s (ERD) report (Harper and Baker, 2015).

With the spatial model domain area expansion, more rainfall stations needed to be included for the development of isopleth data to represent monthly rainfall conditions for the southern model extent, particularly St. Lucie, Martin, and Okeechobee counties). Additionally, AEI gained access to KSC and CCAFS rainfall gauges, which provided a denser dataset in the Barrier Islands (the Banana River watershed), where rainfall patterns are often very different than those on the mainland. The total number of rainfall stations increased from 93 stations in the SWIL 4.0 model to 308 stations in the SWIL 5.0 model, an overall increase of 215 stations or 231% (Figure 2).

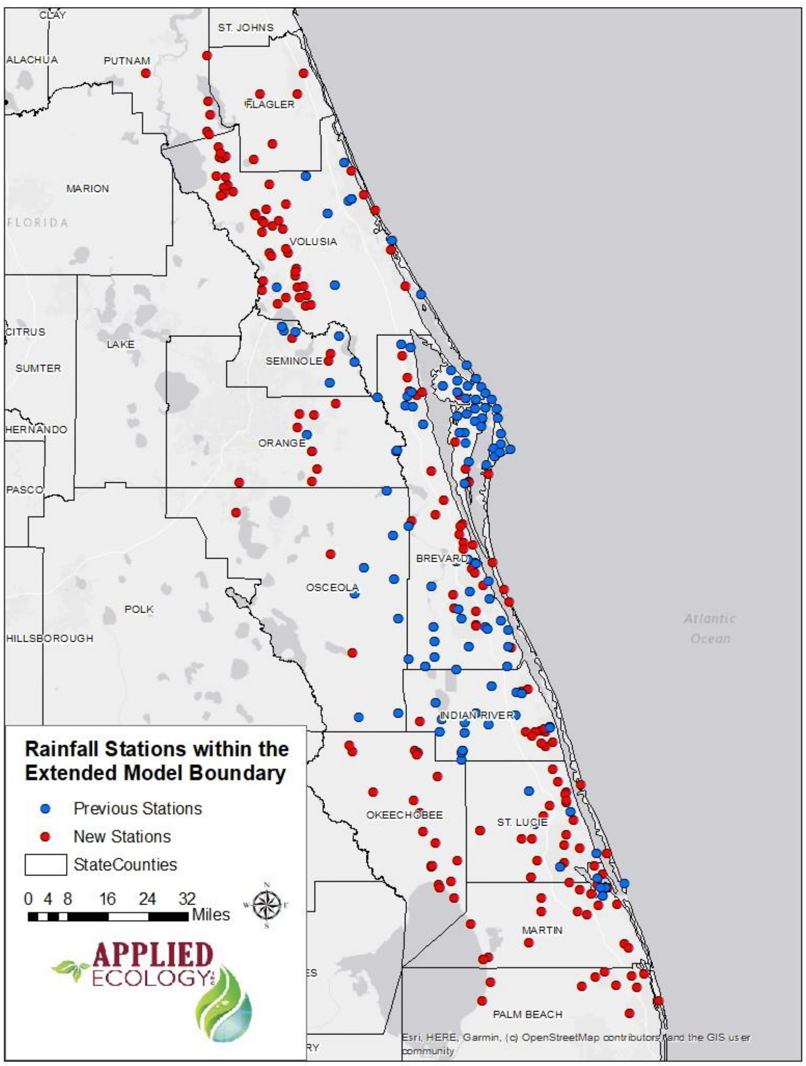


**Figure 2. The increase of the total number of rainfall stations for the SWIL 5.0 model.**

### Evapotranspiration

## Future Land Use Model Modification of the North IRL

### Future Land Use Development

The first modified version of the SWIL 5.0 model was created to determine the impact of future land use changes and anticipate future nutrient loadings into the IRL. This section describes the methodology as well and results of the modified, single-year SWIL model run.

The development of a future land use and treatment GIS coverage for the North IRL watershed was also performed. For most cities and counties, future land use is identified as proposed land use type for 2025; however, the projection could vary and be longer-term for some of the municipalities (which is not necessarily clearly identified).

To accomplish incorporating future watershed land use changes based on current accepted planned development, the first step was to gather all the future land use layers in the North IRL watershed extent. These included two counties (Brevard and Volusia), eight cities (Rockledge, Melbourne, Indian Harbour Beach, Cocoa, Titusville, Indialantic, Edgewater, and Oak Hill), one town (Palm Shores), and the Kennedy Space Center. These layers were either provided in a GIS format or were digitized into a GIS format, based on hardcopy maps. Table 1 describes the specifics of the incoming datasets, formats, and corresponding representative year (if available):

**Table 1. Provider, representative year, and format of the provided datasets used to create future land use.**

| Dataset Provider | Representative Year | Format |
|---|---|---|
| Brevard County | 2025 | Shapefile |
| City of Cocoa | 2020 | Geodatabase |
| City of Edgewater | 2030 | Shapefile |
| City of Melbourne | Not Specified | Shapefile |
| City of Oak Hill | 2025 | Shapefile |
| City of Rockledge | 2025 | Shapefile |
| City of Titusville | Not Specified | Shapefile |
| Kennedy Space Center | 2032 | Geodatabase |
| Town of Indialantic | 2019 | Hardcopy Map |
| Town of Indian Harbour Beach | 2020 | Hardcopy Map |
| Town of Palm Shores | Not Specified | PDF |
| Volusia County | 2025 | Shapefile |

The second step was to examine the future land use codes (which are specific to each municipality) and create lookup tables to convert them to a consolidated system. An example of this process is demonstrated for Brevard County's Future Land Use in Appendix A-2. Some future land use codes included mixed-use parcels, which could be a combination of any of the consolidation codes. These mixed-use parcels were examined individually to determine the most dominant type of land use and converted to the most representative consolidated codes. If the future land use designated areas as "natural", these typically matched with current undeveloped land use types and remained unchanged in our future land use input layer. A seamless future land use layer extending the entire North IRL was created after all land use types had been consolidated into a consistent classification system. The last step was to perform topological and geometry checks on the spatial features using the Validate Topology tool in the ArcGIS Desktop environment. This was done to assure no overlaps, inconsistent classification, or gaps between the polygons were found in this final future NIRL land use coverage.

### Future Treatment Layer Development

In order to predict future land use treatments, future development areas were assigned treatments according to current regulatory requirements. Areas that were converted from one natural or agricultural land use type to another did not receive treatments. Currently treated areas were also maintained in the future land use coverage. All newly added treatment areas were assigned to a dry or wet treatment type. This assignment was based on two assumptions due to limited budget for onsite determination: soil type (hydrologic type A soils were always classified as dry treatments) and location (i.e., within the Barrier Islands often resulted in dry treatments).

### Future Volumes and Nutrient Model Estimate Development

The latest SWIL version was modified for single-year runs using mean POR ET and rainfall raster for each month of the year. Present and future land use and treatment conditions using the one-year model were completed, and outputs were validated for logical consistency. It is important to note that for the future model year condition, mean POR rainfall conditions were used. No modeling or incorporation of predicted future rainfall magnitudes of patterns was incorporated in this task.

## SWIL Model Adaptation for the Military Base Site-Specific Information

In 2016, AEI developed site-specific watershed loading models for the Patrick Air Force Basins (PAFB) and Cape Canaveral Air Force Station (CCAFS). These higher spatial resolution models were developed for the 45th Space Wing (USAF) as part of the Environmental Compliance Program and incorporated the following field-derived datasets: delineated and field validated catchment data, photointerpreted and field validated land use and treatment data, and calculated event mean concentration and runoff coefficients from five years of field-collected stormwater and baseflow. Since both military installations are located within the Banana River Lagoon watershed, changes to the SWIL 5.0 from incorporating these site-specific models only required modifications to the Banana River watershed.

To reduce the level of effort in model processing time and to produce outputs consistent with the most recent FDEP accepted SWIL model for implementation of the Indian River Lagoon Basin Management Action Plan (BMAP), a simplified SWIL was developed (Listopad, 2019). This simplified model, hereafter called the "Aggregated SWIL" model, is the result of converting the Military Site-Specific Models from a dynamic monthly output model to a period-of-record (2004-2017) model. Once converted, The Aggregated SWIL model only needs to be run for 12 months (January to December) to yield representative monthly estimated volumes and nutrient loadings based on recent (2015) land use and soil conditions. To create the Aggregated Baseload SWIL, both rainfall and evapotranspiration data for the representative POR (2004-2017) had to be averaged monthly. Using averaged monthly data greatly improved model performance without impacting the estimated runoff and baseflow volumes and loads.

To ensure the validity of replacing individual monthly raster data for the entire POR (168 months) with aggregated mean values for rainfall and ET, a verification effort was undertaken for each individual military base. Validation was performed of the Aggregated SWIL model by running the original site-specific Military Base Models monthly and averaging the outputs of the 168 monthly runs (Verification SWIL). Results from the Verification SWIL model version run were averaged by month and compared to the results of the Aggregated Baseload SWIL. These results are specific for the two Military Bases (PAFB and CCAFS).

## Rainfall

In order to provide estimated loads that represent variability of rainfall conditions (above and below average rainfall years, different rainfall seasonality patterns, etc.), several years of loading data needed to be simulated for a 10+ year POR; the 2004-2017 POR was chosen, in coordination and agreement with the FDEP, as it represents more recent conditions and captures below normal and above normal rainfall years. This approach is also consistent with other approaches implemented by FDEP for load estimation models used for the needs of the other BMAPs.

Additionally, POR rainfall conditions were aggregated to create 12 representative months to reduce the model run-time. In the previous SWIL model runs, monthly rainfall rasters were created for the POR and loading data were estimated for each of the monthly input data. Aggregation, if any, was performed using the monthly loading outputs. For the baseload estimate development, each monthly rainfall raster between January 2004 and December 2017 was first constructed by interpolating best available rainfall gage data distributed across the IRL area (according to methods described Harper and Baker, 2015, and Applied Ecology, 2015). Subsequently, an average was created for each of the 12 months (e.g., January, February, etc.) based on all 14 years of rainfall data within the selected POR. Aggregated monthly data (12 months only) were used in the Aggregated Baseload SWIL model effort.

## Evapotranspiration

In addition to aggregating the monthly rainfall rasters, the ET rasters were also aggregated by month for the POR (2004-2017). The ET data layers described in the methodology section for the SWIL 5.0 model update were used to construct the ET layers included in the Aggregated Baseload SWIL. As previously stated, the MOD 16 data product is currently only available between the years of 2000-2014. To account for this lapse in data from 2015 to 2017, monthly mean rasters were created to represent the POR in which the measured ET data was available (i.e., the average of identical months for every year from 2000 to 2014). These monthly rasters were then applied to the three subsequent years of the POR with no associated data. Once the data for all years of the POR were created, the aggregated monthly layers were created for the POR of the current SWIL model update (2004–2017). Similar to the rainfall raster datasets, the total number of evapotranspiration input raster layers was reduced from 168 to 12, also decreasing the run-time and increasing efficiency.

# Results

## SWIL 5.0 IRL Watershed

### Land Use Land Cover

Maps of the expanded land use years were created, and summary statistics were performed to determine the amount of increased acreage of each simplified, consolidated land use type for all years of available land use (Table 2 and Figure 3). Topology checks for geometry and logical consistency were performed prior to the model run.

**Table 2. Acreage of each land use type gained from the model extent expansions during the 2000, 2004, and 2015 years.**

| Consolidation Type | Acres Gained in Model Extent Expansion | | |
|---|---|---|---|
| | 2000 | 2004 | 2015 |
| **Agriculture** | 3,059.93 | 3,300.14 | 5,374.83 |
| **Citrus** | 128,927.43 | 121,533.75 | 81,808.47 |
| **Commercial** | 6,314.65 | 7,309.25 | 8,342.33 |
| **Dry Prairie** | 12,488.11 | 16,383.32 | 41,927.44 |
| **High Density Residential** | 27,330.59 | 31,649.64 | 39,228.33 |
| **Hydric Hammock** | 0.00 | 27.91 | 949.70 |
| **Industrial** | 11,517.41 | 11,813.66 | 6,550.38 |
| **Institutional** | 12,657.94 | 13,820.59 | 29,695.12 |
| **Low Density Residential** | 5,839.78 | 5,481.79 | 3,672.65 |
| **Medium Density Residential** | 35,099.60 | 41,928.19 | 39,758.24 |
| **Mesic Flatwoods** | 3,536.13 | 3,289.10 | 1,818.59 |
| **Mining** | 887.12 | 468.59 | 670.75 |
| **Open** | 3,394.31 | 1,748.08 | 1,629.48 |
| **Pasture** | 143,682.23 | 141,087.87 | 120,100.49 |
| **Recreational 1** | 6,295.89 | 6,434.49 | 6,245.70 |
| **Recreational 2** | 794.13 | 916.84 | 1,074.71 |
| **Row Crops** | 11,368.14 | 15,794.69 | 14,743.53 |
| **Ruderal** | 3,436.85 | 1,949.06 | 6,274.77 |
| **Scrub** | 8,712.87 | 5,214.87 | 5,091.45 |
| **Transportation** | 5,057.12 | 5,564.58 | 5,809.78 |
| **Upland Flatwoods** | 5,138.02 | 5,027.51 | 16,487.53 |
| **Upland Mixed** | 348.34 | 283.30 | 5,405.30 |
| **Water** | 43,947.02 | 42,912.26 | 46,496.94 |
| **Wet Flatwoods** | 37,633.69 | 30,410.34 | 28,743.64 |
| **Wet Prairies** | 13,164.68 | 14,944.14 | 12,928.61 |
| **Wetland** | 43,557.50 | 45,164.18 | 43,750.91 |
| **Xeric Hammock** | 956.88 | 688.20 | 566.53 |

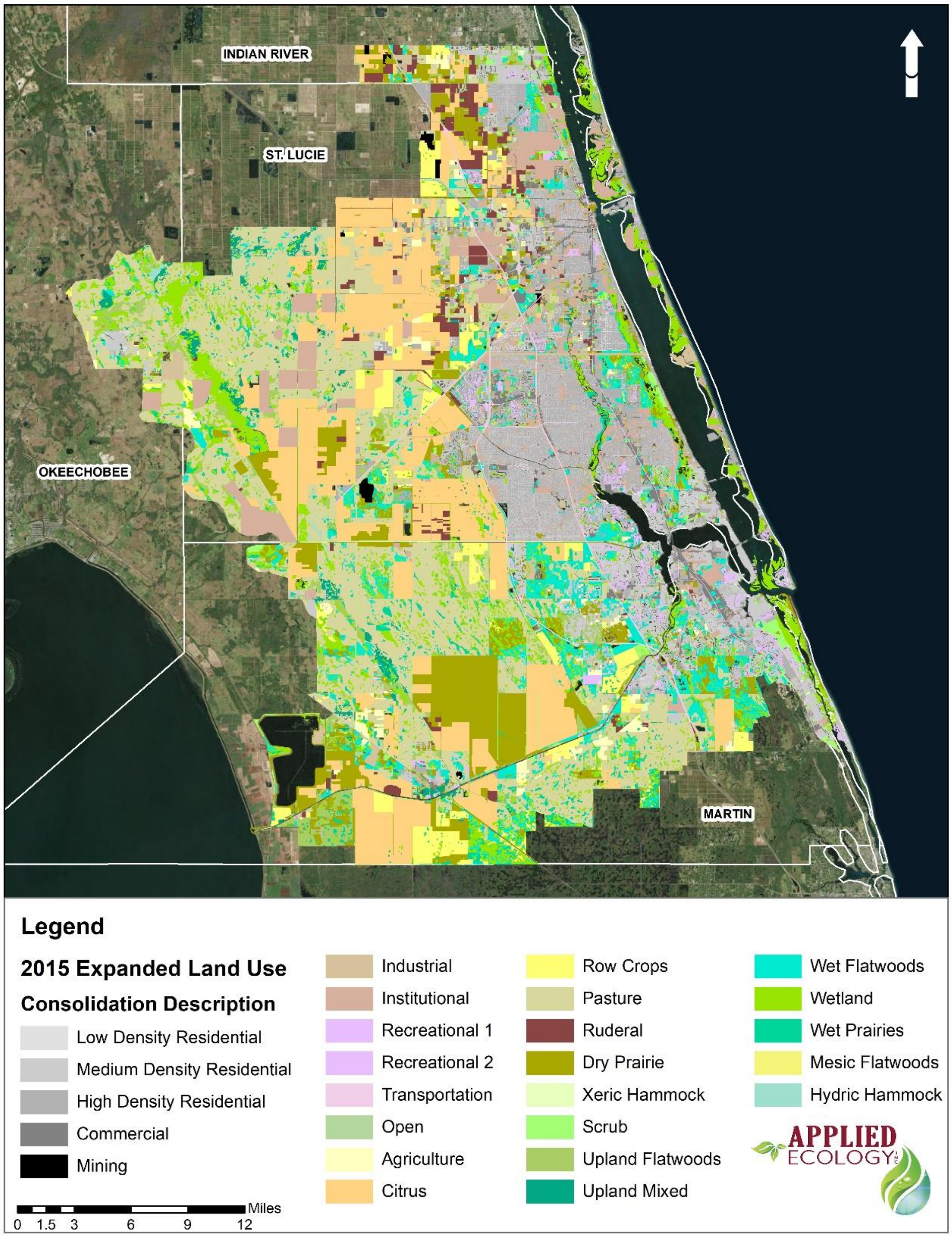


**Figure 3. Distribution of land use consolidation types for the 2015 year for a selected watershed area of the Central and South Indian River Lagoon.**

A comparison of land uses between the three model years (2000, 2004, and 2015) for the entire modeling watershed is provided in Figure 4. To simplify this comparison, all the land uses were grouped into five categories: agriculture, developed (urban), natural (upland and wetland), water (natural and retention ponds), and other (disturbed land, spoil islands, etc.). The most noticeable overall changes are a decrease in agricultural acreage between 2000 (390,315 acres) and 2015 (298,618 acres) and an increase in developed acreage between 2000 (262,132 acres) and 2015 (343,918 acres). Interestingly, the total model area classified as natural has slightly increased from the year 2000 (398,699 acres) to 2015 (405,063 acres). Total model extent covered by water (most likely wet detention ponds typically associated with urbanization) increased from 254,284 to 259,477 acres from 2000 to 2015.

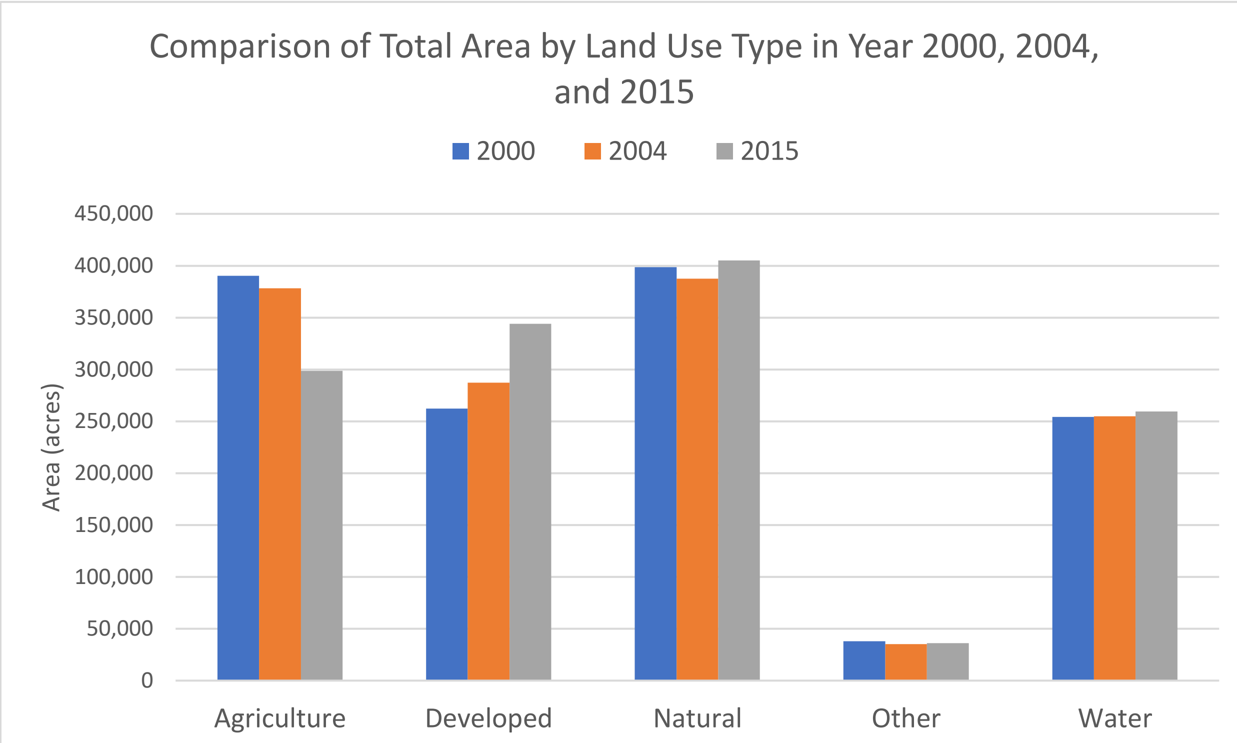


**Figure 4. Comparison of total area, in acres, by land use type for the model years 2000, 2004, and 2015.**

It was surprising to see a slight increase in natural land uses. Some of the basins with the largest increases in natural land use were photointerpreted for quality assurance. In southern St. Lucie County, for example, land use conversion (or abandonment) from agricultural to a more natural state is visible between 2000 and 2015 (Figure 5 and Figure 6). The majority of the agricultural land use conversion, however, has resulted in urban land uses and not semi-ruderal natural habitat.

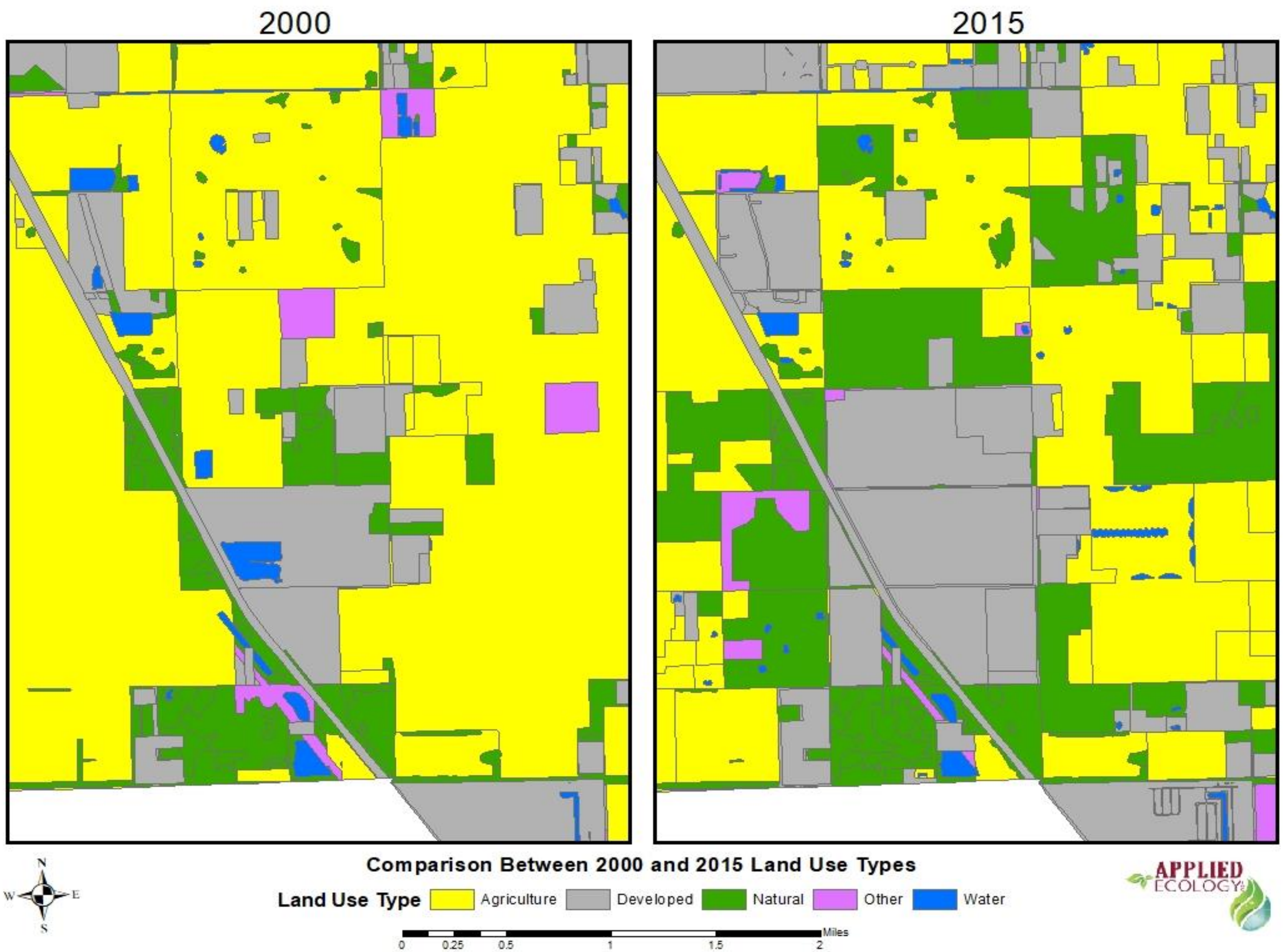


**Figure 5. Comparison of land use type for the years 2000 and 2015, in southern St. Lucie County.**

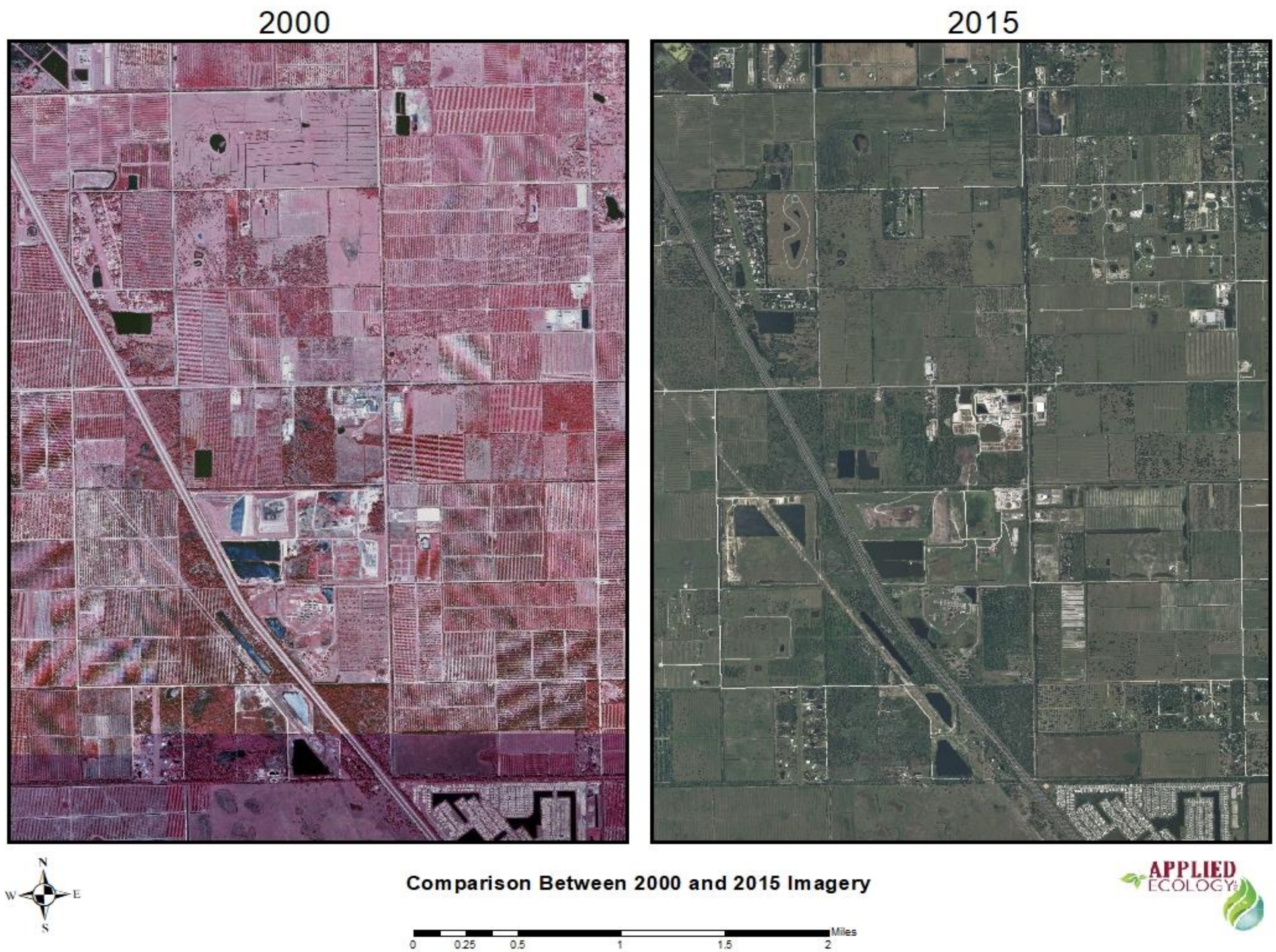


**Figure 6. Comparison of imagery for the years 2000 and 2015, in southern St. Lucie County.**

## Treatments

In Table 3 and Table 4, the acres are compared between the SWIL 4.0 model and the SWIL 5.0 model. The 2000 treatment acreage was increased by 17,750 acres (6,068 dry treatment acres and 11,683 wet treatment acres), the 2004 treatment acreage was increased by 22,559 acres (6,946. dry treatment acres and 15,613 wet treatment acres), and the 2015 treatment acreage was increased by 30,270 acres (8,407 dry treatment acres and 21,863 wet treatment acres). The 2000 and 2004 treatment acres increased by 50%, and the 2015 treatment acres increased by 39%.

**Table 3. The total treatment, wet treatment, and dry treatment acreage of 2000, 2004, and 2015 treatments for SWIL 4.0.**

| Year | Total (Acres) | Dry Treatment (Acres) | Wet Treatment ( Acres) |
|---|---|---|---|
| **2000** | 35,528.17 | 21,295.91 | 14,232.27 |
| **2004** | 45,398.86 | 26,365.02 | 19,033.84 |
| **2015** | 78,524.49 | 33,443.18 | 45,081.31 |

**Table 4. The total treatment, wet treatment, and dry treatment acreage of 2000, 2004, and 2015 treatments for SWIL 5.0. This includes an expanded watershed area.**

| Year | Total (Acres) | Dry Treatment (Acres) | Wet Treatment (Acres) |
|---|---|---|---|
| **2000** | 53,278.39 | 27,363.46 | 25,941.94 |
| **2004** | 67,957.97 | 33,311.52 | 34,646.46 |
| **2015** | 108,794.56 | 41,850.35 | 66,944.21 |

## Soils

Similar to the SWIL 4.0 Model, the resulting soils were comprised predominantly of the "A/D" and "C/D" dual groups (33.14% and 24.18% respectively) and the least common soil types were "C" and "B" types of soil, which combined only represented less than 0.3% of all the model domain soils (Figure 7, Table 5).

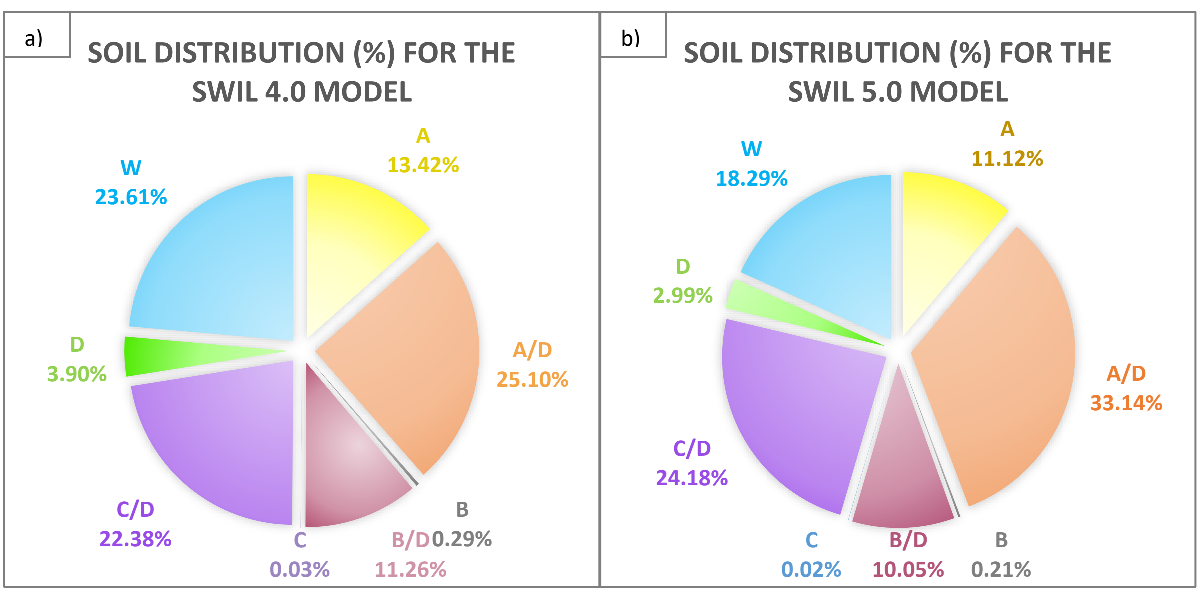


**Figure 7. Distribution of soil types for the (a) SWIL 4.0 Model and (b) SWIL 5.0 Model.**

There was on overall increase of 407,603 acres after the model boundary was expanded, with the largest increase observed in the "A/D" soil type (89.51%) and the lowest increase in the "B" soil type (0.93%) (Table 5).

**Table 5. Total acreage of each soil type for the SWIL 4.0 and SWIL 5.0 Model runs as well as the increase, in acres and percent, from the SWIL 4.0 to the SWIL 5.0 Model run.**

| Soil Type | SWIL 4.0 Acres | SWIL 5.0 Acres | Increase (Acres) | Increase (%) |
|---|---|---|---|---|
| **A** | 125,599 | 149,423 | 23,824 | 18.97 |
| **A/D** | 234,878 | 445,111 | 210,233 | 89.51 |
| **B** | 2,741 | 2,766 | 25 | 0.93 |
| **B/D** | 105,400 | 135,036 | 29,636 | 28.12 |
| **C** | 255 | 321 | 66 | 25.72 |
| **C/D** | 209,440 | 324,780 | 115,340 | 55.07 |
| **D** | 36,460 | 40,101 | 3,641 | 9.99 |
| **W** | 220,881 | 245,720 | 24,839 | 11.25 |
| **Total:** | 935,655 | 1,343,258 | 407,603 | 43.56 |

## Rainfall

Datasets for all 334 stations were downloaded, organized, and prepared with data up to and including December 2017. Stations with incomplete data for each month of interest were excluded using custom queries and filters from the raster generation process. Monthly rainfall isopleths (in raster format) were generated with complete data for each specific month of interest (January 1995 to December 2017). An example of a newly generated monthly raster is provided in Figure 8.

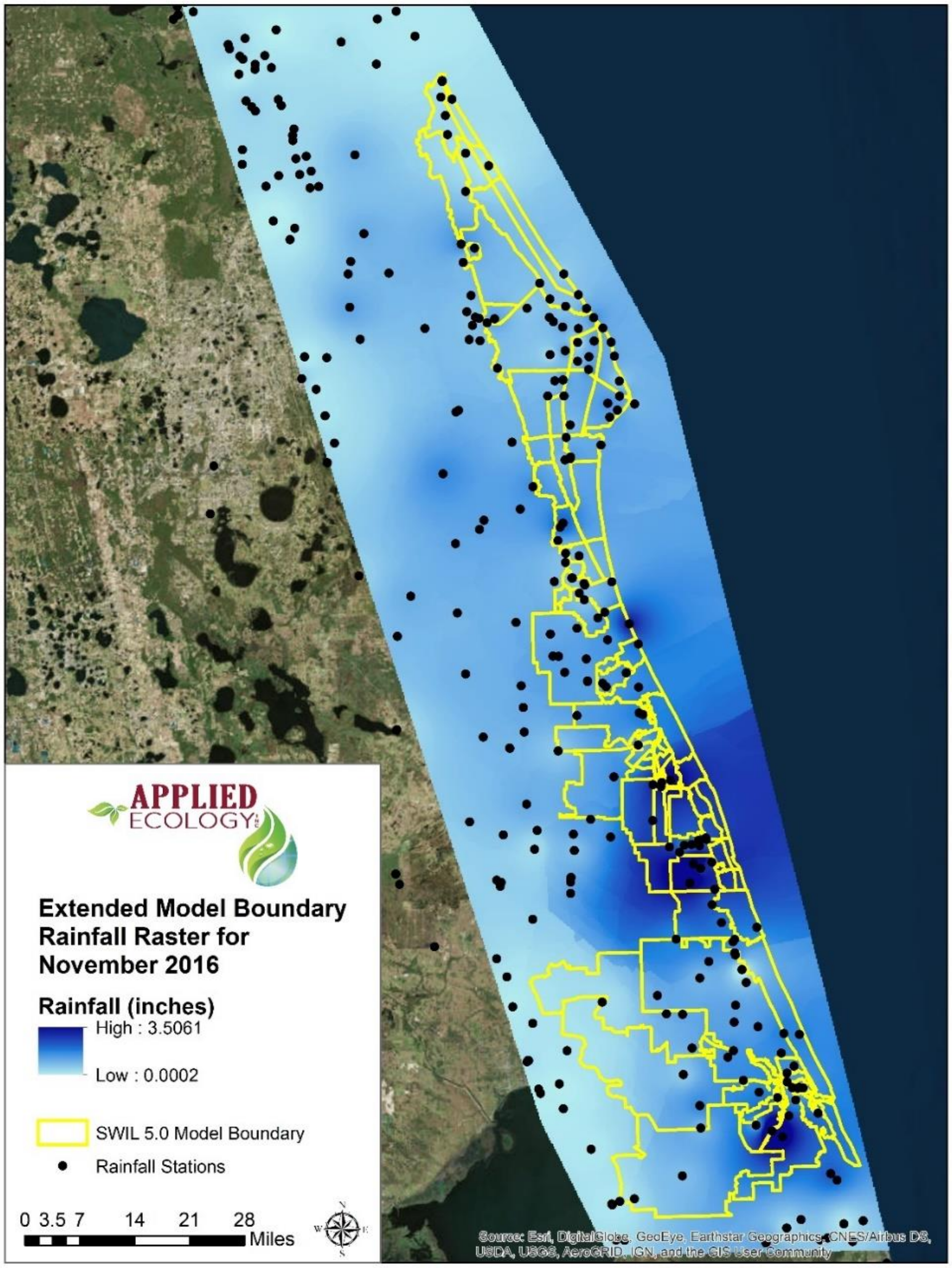


**Figure 8. Rainfall raster for November 2016 throughout the SWIL 5.0 Model**

Not all 334 stations had available and complete information for every month of the 1995-2017 model period. SWIL 5.0 used up to 164 stations per month to generate new rainfall isopleth raster dataset to cover the entire spatial model domain.

Average rainfall for each of the sublagoons for the SWIL 4.0 model and the SWIL 5.0 model was calculated for comparison purposes. Table 6 and Table 7 reflect the differences in rainfall throughout the period of record due to the increase in the number of rainfall stations. Cells that represent increases of 2” or greater are highlighted in blue and those with decreases of 2” or greater in orange for better visualization of significant changes in the rainfall input layer for SWIL 5.0. Changes in rainfall drive estimated volumes, which have a direct impact on the total nutrient loading to the lagoon. Most of the changes reported from increasing the rainfall gauge network were demonstrated as increases in rainfall in the 2-3” range. For example, the Mosquito Lagoon watershed had some significant increases in rainfall (1996) with the addition of many Kennedy Space Center gauge information.

**Table 6. Comparison of the POR average rainfall (in inches) for the Banana River and Central IRL sublagoons for SWIL 4.0 and SWIL 5.0.**

| Sublagoon | Banana River | | Central IRL | |
|---|---|---|---|---|
| **Model** | **SWIL 4.0** | **SWIL 5.0** | **SWIL 4.0** | **SWIL 5.0** |
| **1995** | 52.63 | 56.19 | 52.88 | 53.85 |
| **1996** | 50.23 | 52.30 | 52.60 | 54.95 |
| **1997** | 56.69 | 48.44 | 60.58 | 62.27 |
| **1998** | 44.43 | 41.82 | 52.61 | 56.28 |
| **1999** | 59.09 | 57.55 | 54.02 | 54.03 |
| **2000** | 33.31 | 31.58 | 39.02 | 40.22 |
| **2001** | 59.20 | 51.99 | 52.87 | 53.59 |
| **2002** | 52.93 | 45.97 | 52.37 | 54.64 |
| **2003** | 43.84 | 42.47 | 44.79 | 46.03 |
| **2004** | 51.54 | 50.94 | 53.97 | 55.61 |
| **2005** | 58.48 | 60.61 | 55.26 | 57.14 |
| **2006** | 31.91 | 33.23 | 33.89 | 34.06 |
| **2007** | 49.14 | 46.76 | 44.44 | 45.62 |
| **2008** | 59.59 | 60.51 | 54.78 | 56.55 |
| **2009** | 39.91 | 41.93 | 42.72 | 44.13 |
| **2010** | 37.95 | 40.68 | 39.19 | 40.49 |
| **2011** | 44.47 | 47.61 | 51.59 | 53.33 |
| **2012** | 42.56 | 39.58 | 44.81 | 47.37 |
| **2013** | 38.91 | 36.99 | 46.63 | 48.06 |
| **2014** | 53.94 | 54.14 | 54.36 | 58.54 |
| **2015** | 33.30 | 50.81 | 30.05 | 51.77 |
| **2016** | | 55.00 | | 62.33 |
| **2017** | | 61.91 | | 67.52 |

**Table 7. Comparison of the POR average rainfall (in inches) for the Mosquito Lagoon, North IRL, and South IRL sublagoons for SWIL 4.0 and SWIL 5.0.**

| Sublagoon | Mosquito Lagoon | | North IRL | | South IRL |
|---|---|---|---|---|---|
| Model | SWIL 4.0 | SWIL 5.0 | SWIL 4.0 | SWIL 5.0 | SWIL 5.0 |
| 1995 | 52.86 | 54.70 | 52.78 | 56.22 | 60.54 |
| 1996 | 46.75 | 54.96 | 49.36 | 52.31 | 50.68 |
| 1997 | 46.10 | 44.65 | 57.81 | 55.11 | 56.02 |
| 1998 | 39.87 | 38.82 | 46.61 | 45.24 | 62.22 |
| 1999 | 47.89 | 45.99 | 55.40 | 55.72 | 56.80 |
| 2000 | 33.77 | 33.17 | 35.39 | 35.01 | 39.01 |
| 2001 | 62.22 | 61.02 | 60.26 | 60.24 | 59.54 |
| 2002 | 52.25 | 49.19 | 52.04 | 49.53 | 42.72 |
| 2003 | 47.01 | 46.29 | 43.10 | 43.03 | 47.22 |
| 2004 | 49.14 | 50.06 | 51.36 | 52.32 | 53.31 |
| 2005 | 52.52 | 52.12 | 55.70 | 57.98 | 56.45 |
| 2006 | 31.54 | 33.27 | 33.34 | 36.22 | 34.41 |
| 2007 | 42.86 | 41.07 | 46.7 | 46.57 | 57.15 |
| 2008 | 46.95 | 47.90 | 57.18 | 58.37 | 59.06 |
| 2009 | 47.51 | 49.28 | 42.38 | 44.78 | 34.54 |
| 2010 | 34.42 | 36.14 | 37.52 | 40.69 | 46.90 |
| 2011 | 43.16 | 45.17 | 46.6 | 49.96 | 47.13 |
| 2012 | 39.90 | 40.84 | 43.18 | 43.37 | 51.03 |
| 2013 | 40.87 | 42.03 | 41.06 | 41.44 | 51.86 |
| 2014 | 60.80 | 64.00 | 57.04 | 60.71 | 54.42 |
| 2015 | 26.05 | 40.58 | 33.54 | 49.25 | 49.92 |
| 2016 | | 45.43 | | 53.50 | 56.58 |
| 2017 | | 48.00 | | 63.89 | 61.42 |

## Volumes and Nutrient Loading Estimates

The SWIL 5.0 model was run to estimate watershed loadings. A brief summary of the SWIL 5.0 watershed loading estimations is provided in this section. Figure 9 presents the total annual predicted volume for the entire modeled watershed. The combined South IRL and St. Lucie River watershed, being the largest in total area, provides the largest total volumes, followed by the Central IRL, the North IRL, the South IRL, the Banana River, and the Mosquito Lagoon watershed.

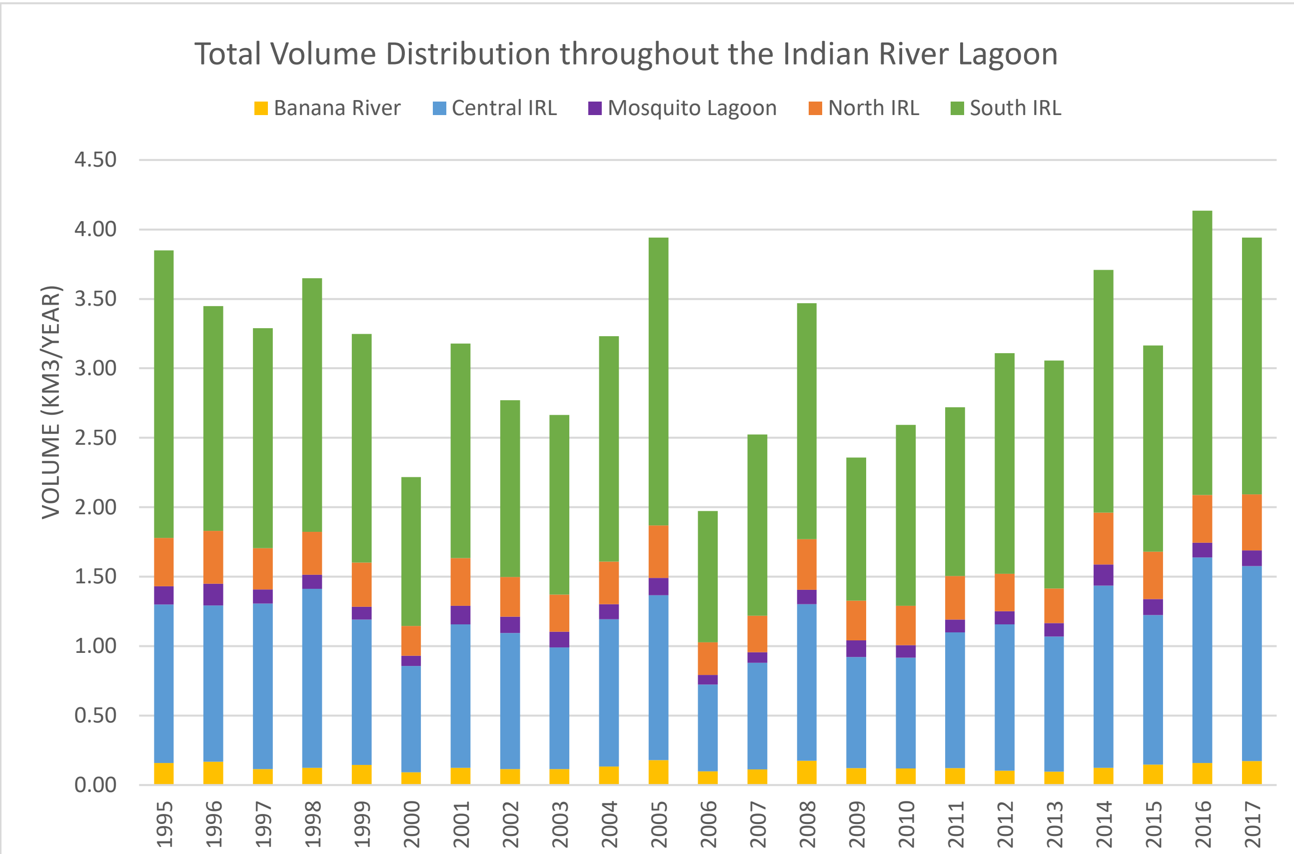


**Figure 9. Interannual variation of the total predicted volumes for each of the IRL Sublagoons.**

Across the Indian River Lagoon watershed, the distribution of the runoff volumes is dominated by baseflow volumes making up about 60-70% of the total volumes. The baseflow contribution to the total volumes per Sublagoon is greater for the Banana River, the Central IRL and SIRL, and less pronounced for the Mosquito Lagoon and North IRL (Figure 10). The interannual variation is similar for most of the sublagoons, with consistently lowest estimated annual volumes for both 2000 and 2006. However, the patterns are slightly different for the highest volume producing years depending on the sublagoon: 2005 and 2008 produce the highest volumes for the Banana River, 2016 and 2017 are the highest volume years for the Central IRL, 1996 and 2014 are the highest for the Mosquito Lagoon, 2017 is the highest for the North IRL, and 1995, 2005, and 2016 are the highest for the South IRL (Figure 10).

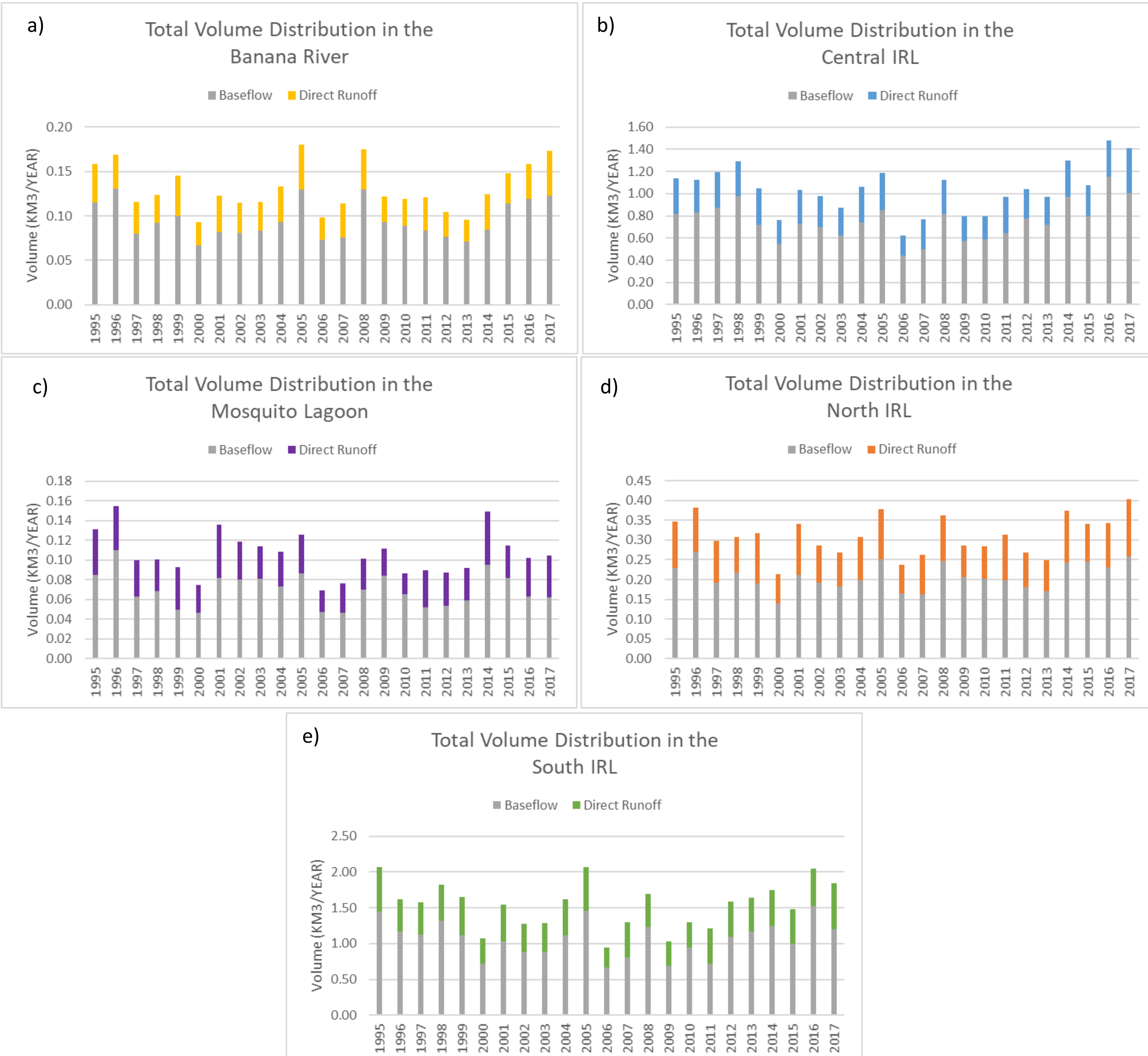


**Figure 10. Interannual variation of the baseflow and runoff predicted volumes for each of the IRL Sublagoons: a) Banana River, b) Central IRL, c) Mosquito Lagoon, d) North IRL, and e) South IRL/St. Lucie.**

The pattern for the total nitrogen (TN) and total phosphorus (TP) loadings are very similar to the predicted volumes for the entire watershed, both in terms of watershed interannual distribution (Figure 11 and Figure 12) and distribution of baseflow/direct runoff (Figure 13 and Figure 14). The years that are predicted to have the lowest loading of nutrients into the lagoon are 2000 (annual watershed-wide rainfall in between 32”-40”), and 2006 (33-34” annual rainfall). The years predicted to have the highest loadings into the lagoon are 2005, 2016, and 2017, all years with large tropical storm/hurricane impacts. Even though the contribution of baseflow loadings to the total lagoon loadings is still significant, it makes up only 50-60% of the total estimated loadings depending on the nutrient and the specific Sublagoon (Figure 13 and Figure 14).

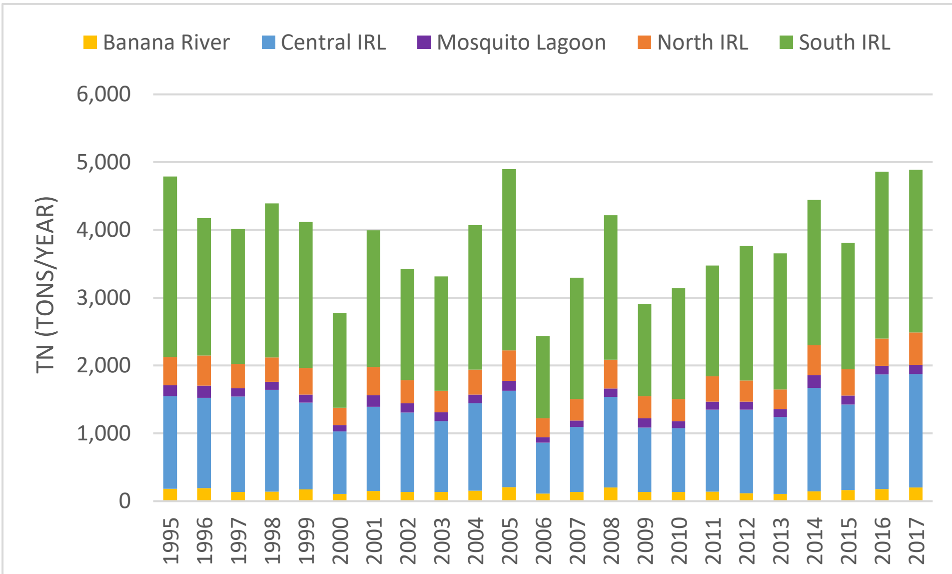


**Figure 11. Interannual variation of the total predicted TN loadings for each of the IRL Sublagoons.**

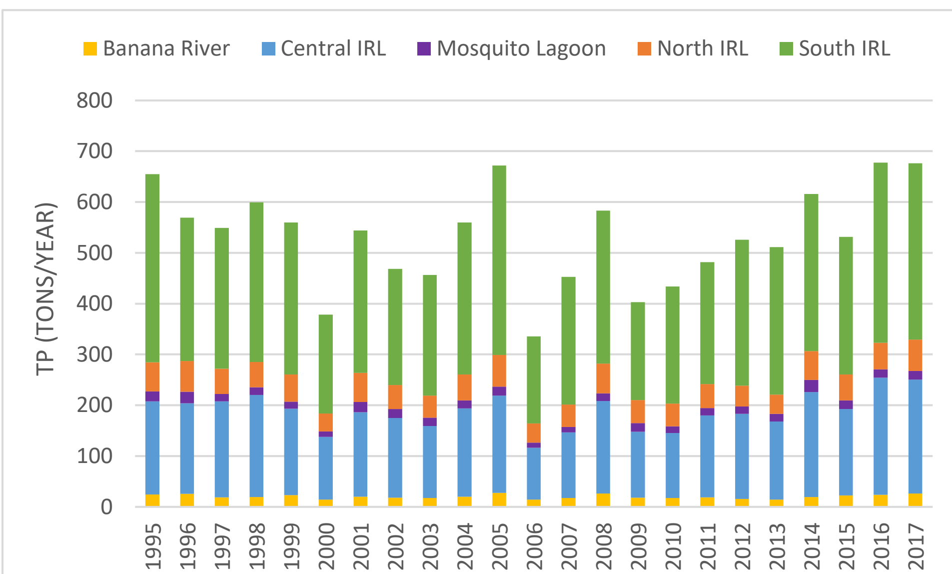


**Figure 12. Interannual variation of the total predicted TP loadings for each of the IRL Sublagoons.**


**Figure 13. Interannual variation of the baseflow and runoff predicted total nitrogen loading for each of the IRL Sublagoons: a) Banana River, b) Central IRL, c) Mosquito Lagoon, d) North IRL, and e) South IRL.**

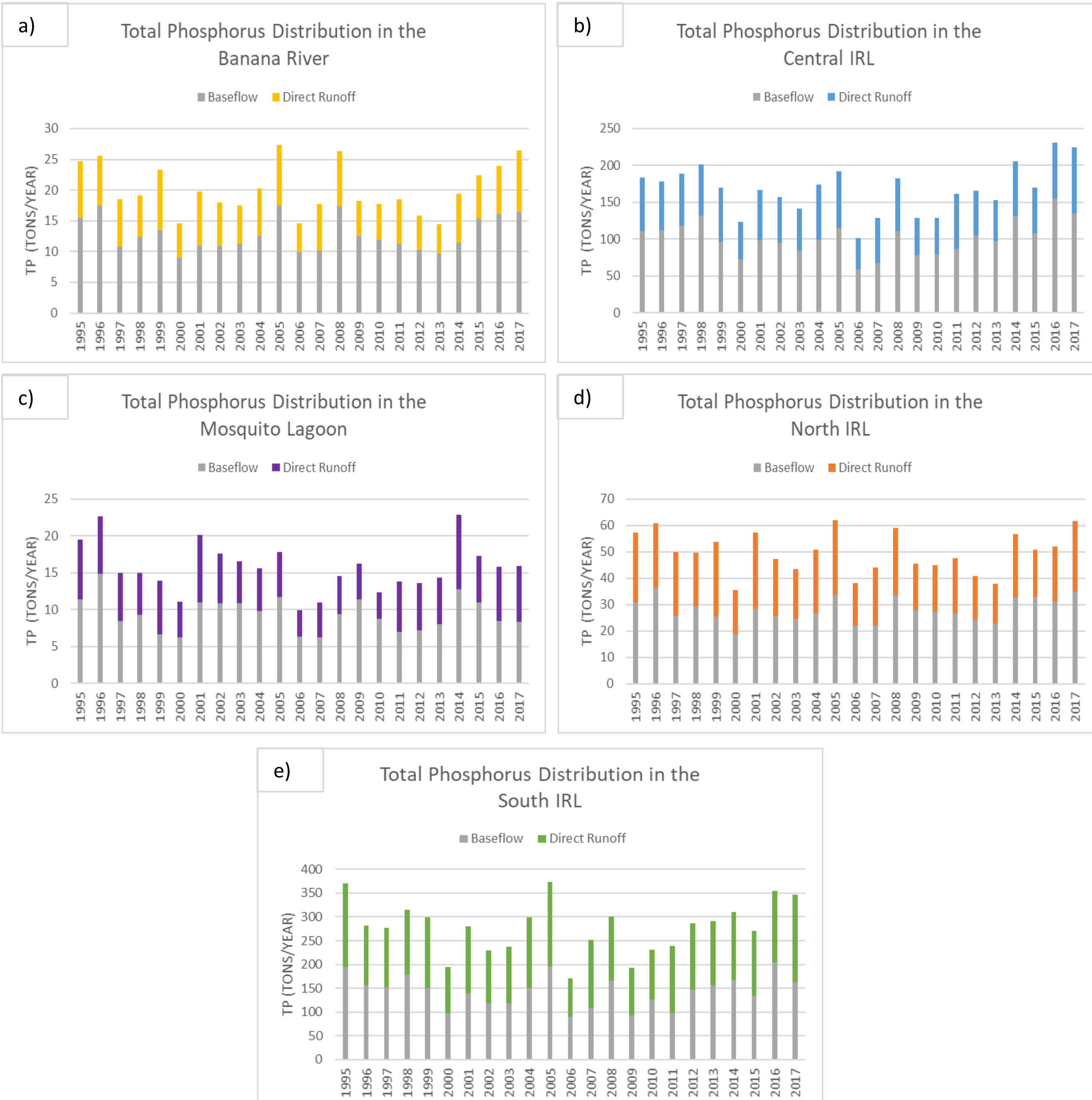


**Figure 14. Interannual variation of the baseflow and runoff predicted total phosphorus loading for each of the IRL Sublagoons: a) Banana River, b) Central IRL, c) Mosquito Lagoon, d) North IRL, and e) South IRL.**

The spatial distribution of the predicted volumes, TN loadings, and TP loadings can be visualized in Figure 15 through Figure 17. For each of these predicted variables, the annual period of record mean and seasonal (January-May totals) were provided as “a” and “b” versions of the map. No normalization by area was included in this spatial visualization: basins with larger areas are expected to have higher volume and loading potential than smaller basins if soil type and urbanization intensity are similar.

As expected, the total volume, TN and TP loading annual means are over three times higher than the seasonal mean corresponding values. The spatial pattern is similar for both predicted volumes and loadings annually and seasonally. There are several consistent hotspots, one in the Central IRL (IR-12 or Turkey Creek catchment) and four in the South IRL (C-44, C23, C24, and St. Lucie North Fork). There are six basins that show an above average contribution of volumes; they include one in the North IRL (IR5), three in the Central IRL (IR14-15-I, IR16-20-D, and IRL-Basin1), and one in the South IRL (South Fork).

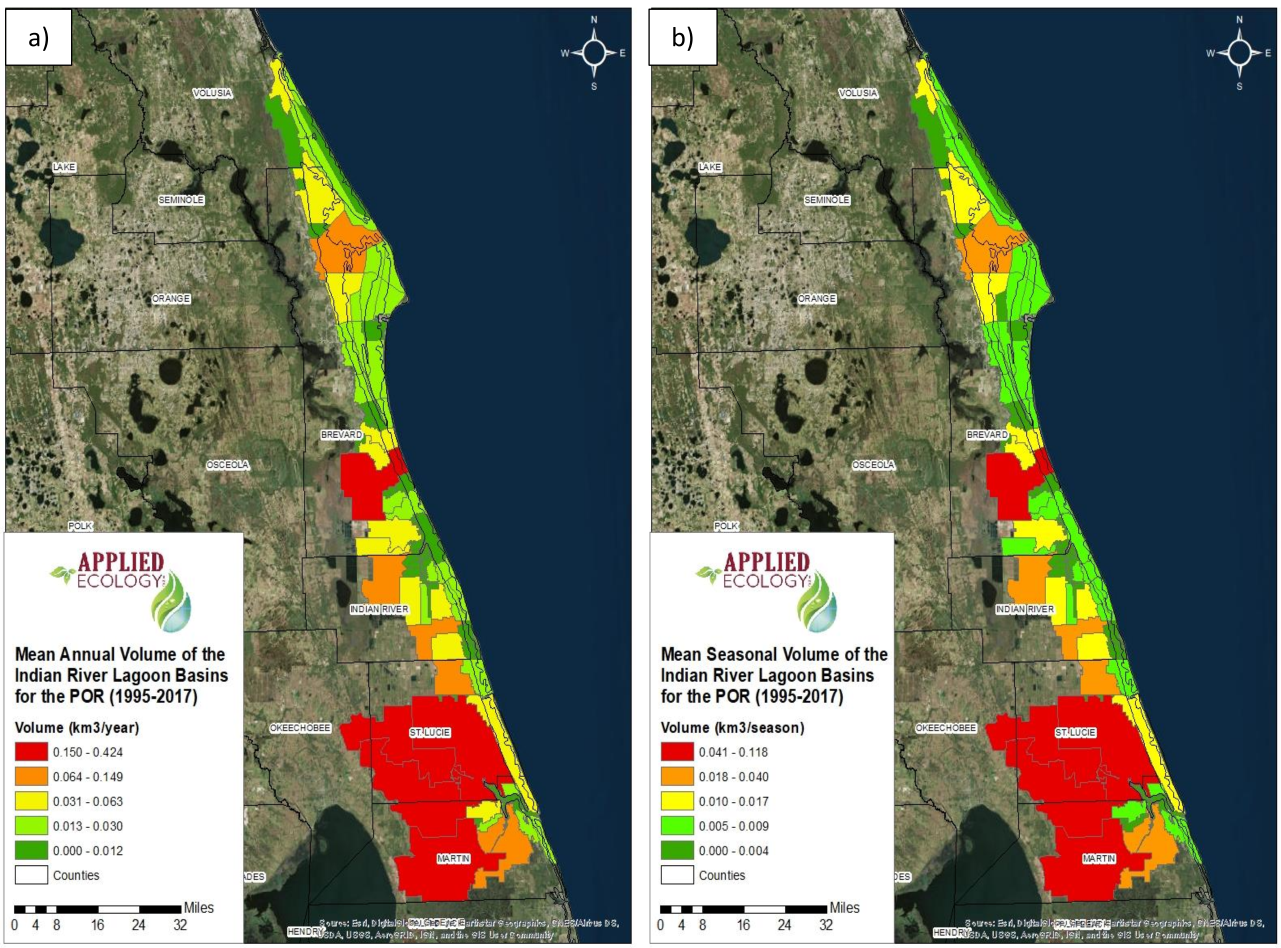


**Figure 15. (a) Distribution of the mean annual total volume throughout the IRL subbasins for the period of record (1995-2017). (b) Distribution of the mean seasonal (January to May) total volume throughout the IRL subbasins for the period of record (1995-2017).**

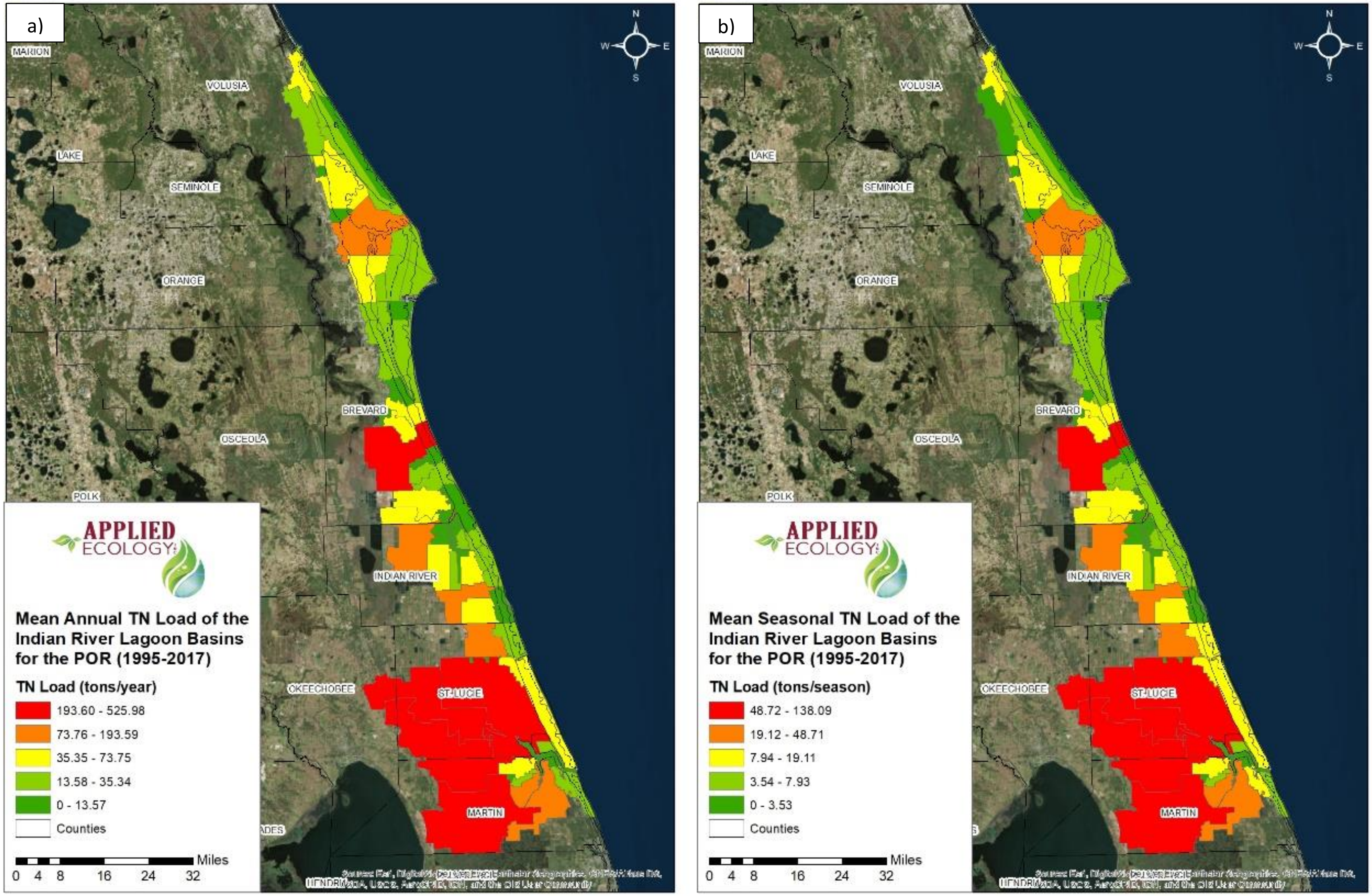


**Figure 16. (a) Distribution of the mean annual total nitrogen load throughout the IRL subbasins for the period of record (1995-2017). (b) Distribution of the mean seasonal (January to May) total nitrogen load throughout the IRL subbasins for the period of record**

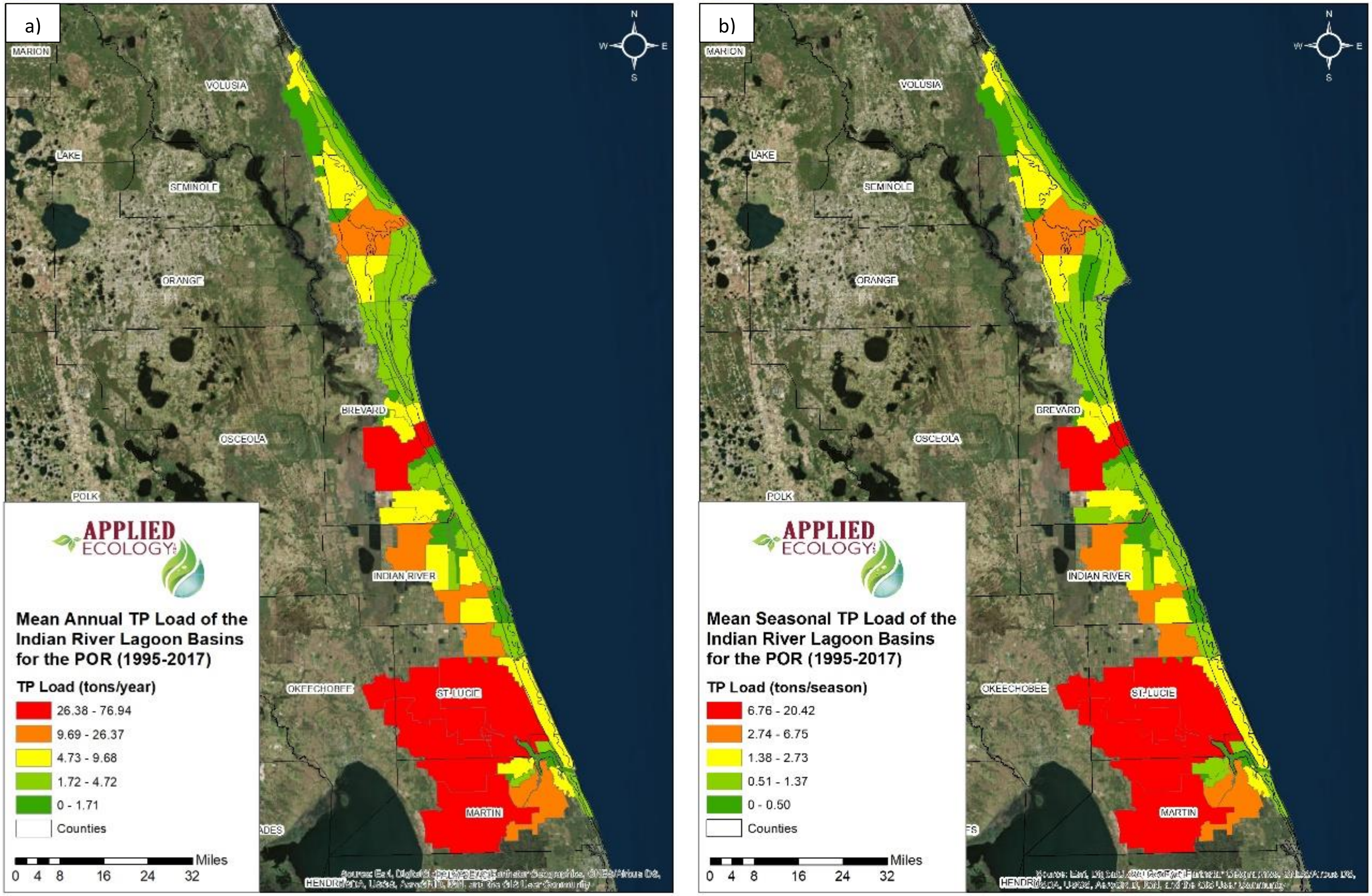


**Figure 17. (a) Distribution of the mean annual total phosphorus load throughout the IRL subbasins for the period of record (1995-2017). (b) Distribution of the mean seasonal (January to May) total phosphorus load throughout the IRL subbasins for the period of record**

There are many areas of the lagoon's watershed that appear to have relatively lower input volumes and loadings to the IRL: these include portions of the Mosquito Lagoon, North IRL, most of the Banana River, and smaller basins in the Central IRL. Most of the basins in the BR and CIRL are smaller watersheds, and normalization might allow a better comparison of the intensity of loading per basin acre. Nevertheless, the larger hotspot basins should be closely monitored for potential water quality impacts on the lagoon.

## Future Land Use Modeling of the North IRL

### Future Land Use Results

To simplify the comparison between current and predicted future land use conditions, the typical model-based consolidated categories (28 different codes) into one of five land use types (developed, agriculture, natural, other, and water). Changes in land use for the North Indian River Lagoon watershed between current and future predicted land use are substantial, particularly for the developed land use types (Figure 18). An estimated increase of 103% in developed land use codes (from 44,345 to 90,186 acres) is accompanied by a decrease in natural land uses of 48% (from 79,143 to 41,330 acres).

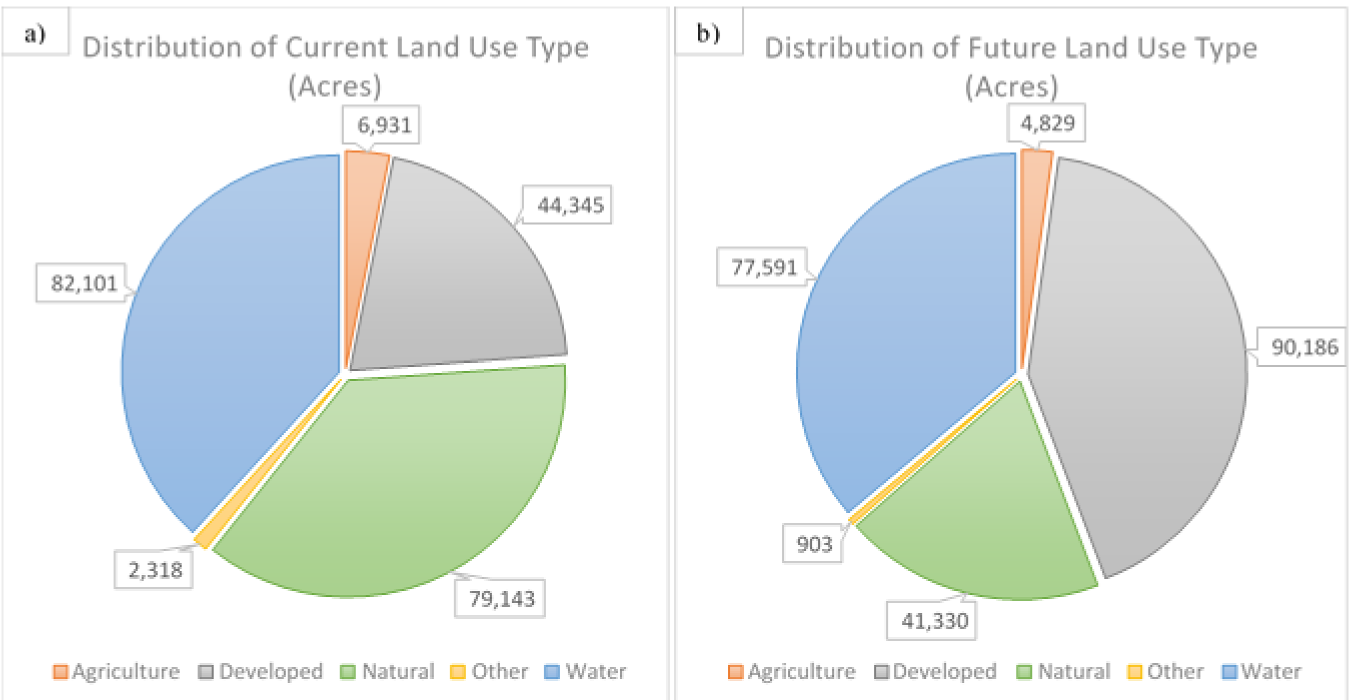


**Figure 18. Distribution of major land use types for the North IRL watershed for (a) current land use and (b) future land use.**

Figure 19 provides an example of the typical land use changes observed between current and future land use for one watershed basin with the North IRL (IR6-7-A and IR6-7-B basins). This basin clearly shows the conversion of natural and agricultural (rangeland/ruderal) to residential and commercial developed land.

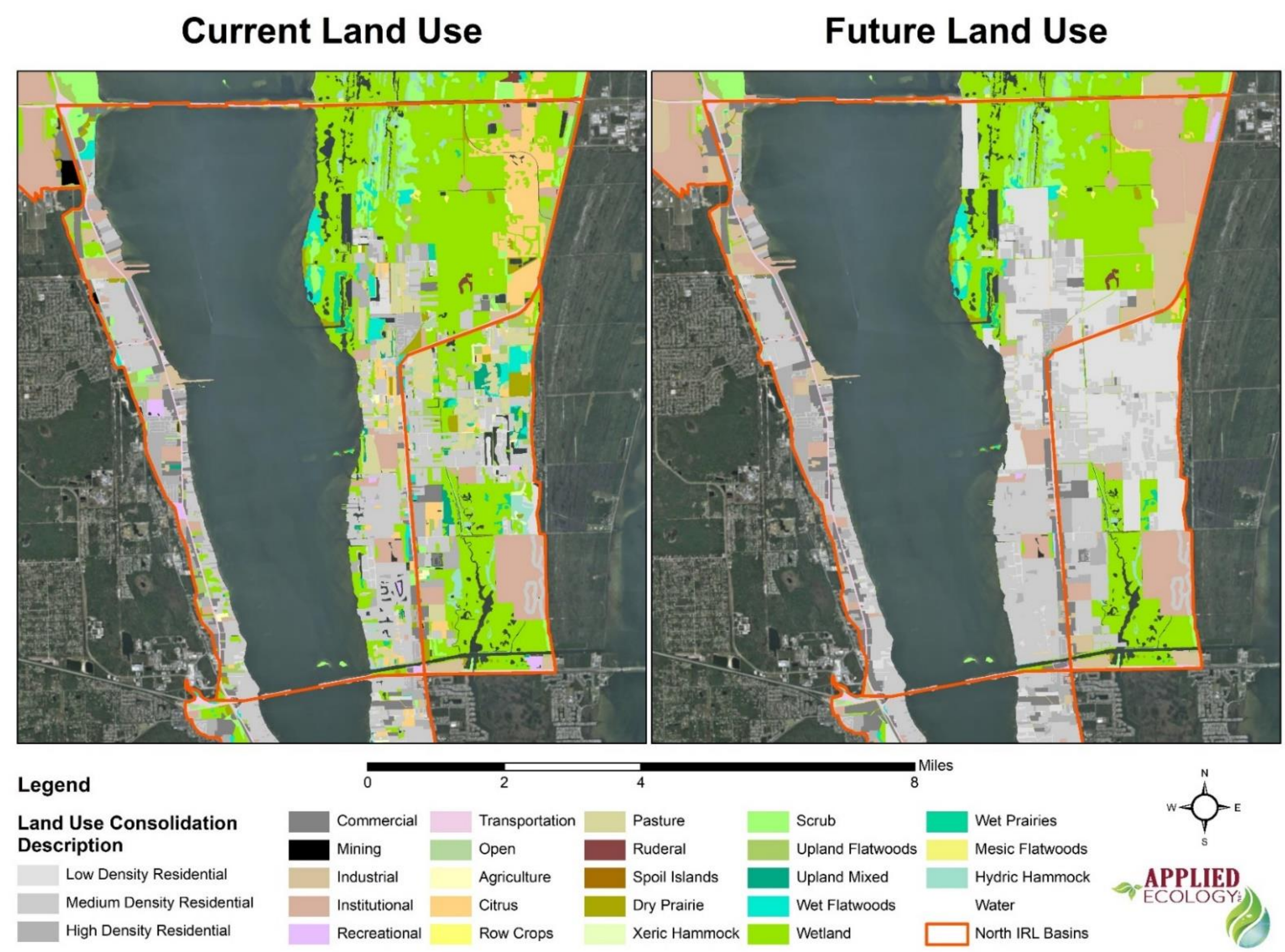


**Figure 19. Distribution of land use consolidation types for the current land use year (2015) and future land use year (2025) the for the IR6-7-A and IR6-7-B basins within the North Indian River Lagoon. Increases in the urban areas are visible with the expansion of the grey colors (urban residential and commercial uses).**

In general, most basins within the NIRL are predicted to have increases in urban land use types (Figure 20). However, there are five basins which clearly demonstrate a greater urbanization pattern, according to the future land use coverages: IR1-3-B, IR5, IR1-3_Big_Flndr, IR1-3-A, and IR6-7-B (with increases of 567%, 191%, 153%, 125%, and 101% of urban area). The conversion to urban areas implies a decrease across most of the basins in both agricultural and natural land use types. The only basin that demonstrates an increase in agricultural land use types between current and future conditions is IR1-3-A, with a 204% estimated increase in agriculture land use area.

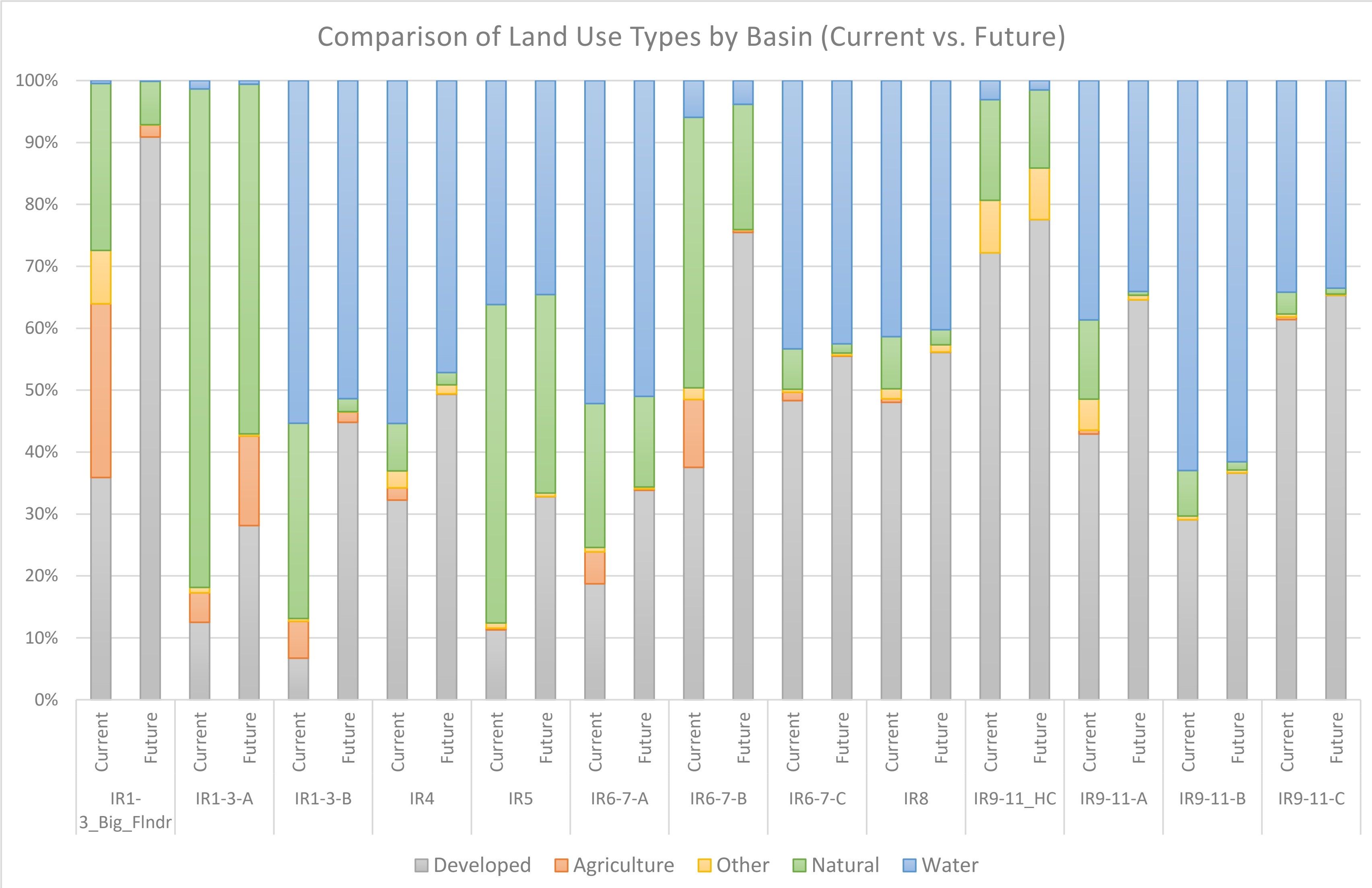


**Figure 20. Distribution of major land use types by basin for current and future land use in the North IRL.**

## Future Treatment Results

As expected, with the expansion of the developed land use type from 2015 to 2025, the treatment area expanded as well. The 2025 treatment area increased by 42,518 acres, with the largest increases observed in the IR1-3-B and IR5 basins (Table 8).

**Table 8. Dry, wet, and total treatment acreages for the current (2015) and future (2025) land use.**

| Basin | Dry | | Wet | | Total | |
|---|---|---|---|---|---|---|
| | *Current* | *Future* | *Current* | *Future* | *Current* | *Future* |
| ***IR1-3_Big_Flndr*** | 148.66 | 156.29 | 0.00 | 1,011.05 | 148.66 | 1,167.34 |
| ***IR1-3-A*** | 131.32 | 969.60 | 977.85 | 4,345.42 | 1,109.17 | 5,315.02 |
| ***IR1-3-B*** | 485.01 | 1,034.17 | 474.23 | 15,591.08 | 959.24 | 16,625.24 |
| ***IR4*** | 293.67 | 423.37 | 412.57 | 1,129.74 | 706.24 | 1,553.11 |
| ***IR5*** | 1,346.35 | 1,751.17 | 494.68 | 12,701.98 | 1,841.03 | 14,453.15 |
| ***IR6-7-A*** | 1,049.87 | 1,505.58 | 1,143.22 | 4,129.92 | 2,193.09 | 5,635.49 |
| ***IR6-7-B*** | 537.21 | 550.77 | 599.92 | 2,773.12 | 1,137.13 | 3,323.88 |
| ***IR6-7-C*** | 404.33 | 614.71 | 198.46 | 393.07 | 602.79 | 1,007.78 |
| ***IR8*** | 996.47 | 1,216.77 | 1,154.64 | 1,556.11 | 2,151.11 | 2,772.88 |
| ***IR9-11_HC*** | 416.73 | 436.78 | 871.11 | 928.97 | 1,287.84 | 1,365.75 |
| ***IR9-11-A*** | 1,160.08 | 1,608.29 | 2,449.02 | 2,822.62 | 3,609.10 | 4,430.92 |
| ***IR9-11-B*** | 291.68 | 369.31 | 1,235.55 | 1,482.62 | 1,527.23 | 1,851.93 |
| ***IR9-11-C*** | 1,886.15 | 2,025.72 | 1,112.81 | 1,261.39 | 2,998.96 | 3,287.11 |

## Future NIRL Volume and Nutrient Loading Estimates

Across the NIRL watershed, there was an overall increase in the total volume output from the current model year (2015) (0.32 $km^3$) to the future model year (typically designated as 2025 or 2035) (0.38 $km^3$). The distribution of the runoff volumes was dominated by baseflow volumes during both the current model year (67%) and the future model year (76%), with an overall increase of 39% of the baseflow volume (Figure 21). In contrast, direct runoff volumes decreased by 13% (0.01 $km^3$) from current to predicted future land use. The total contribution of baseflow to the total produced watershed volumes might be greatly altered if future rainfall patterns change.

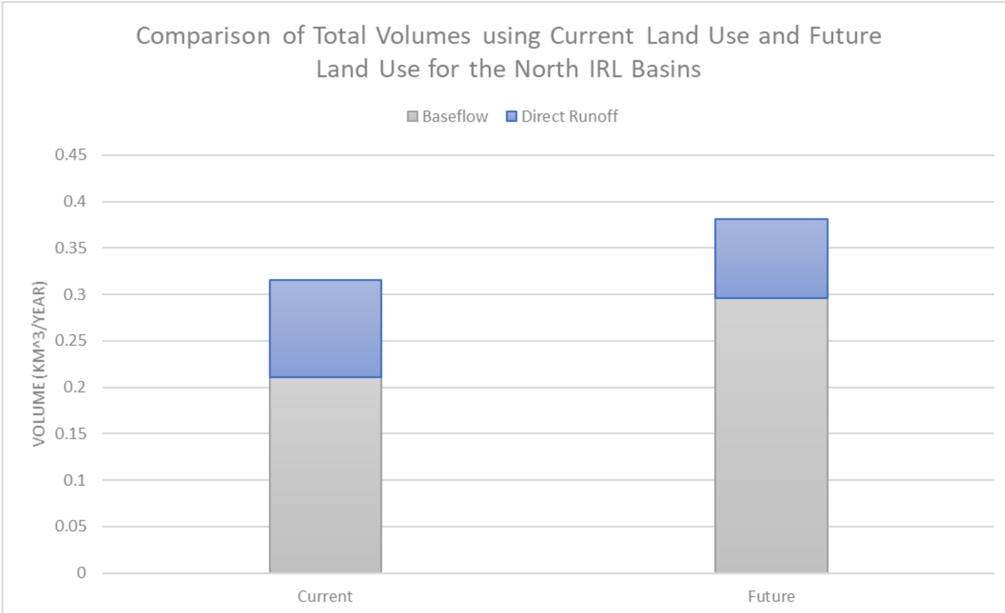


**Figure 21. Predicted baseflow and direct runoff total volumes within the NIRL watershed for both the current model year (2015) and future model year (2025).**

Nutrient loading (TN and TP) estimates from the current model year (2015) to the future model year (2025) increased by 58 and 10 tons, respectively (Figure 22, Figure 23). The distribution of both nutrient runoff loads was dominated by baseflow during both the current model year and the future model year, making up 56%-68% of the estimated nutrients loads into the NIRL, with slightly greater contribution to the total loading for the future model year run.

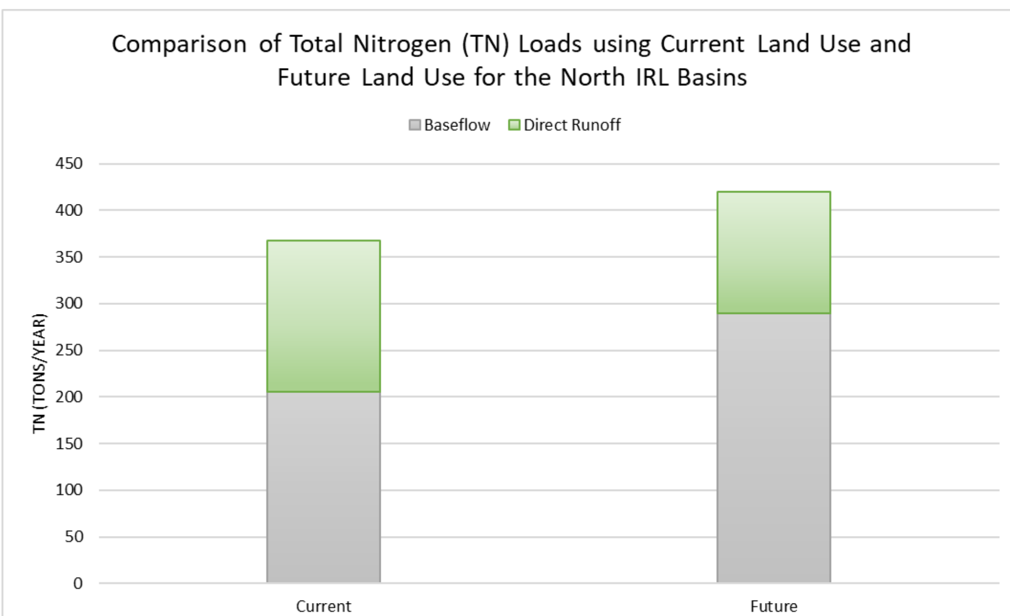


**Figure 22. Predicted baseflow and direct runoff TN loads within the NIRL watershed for both the current model year (2015) and future model year (2025).**

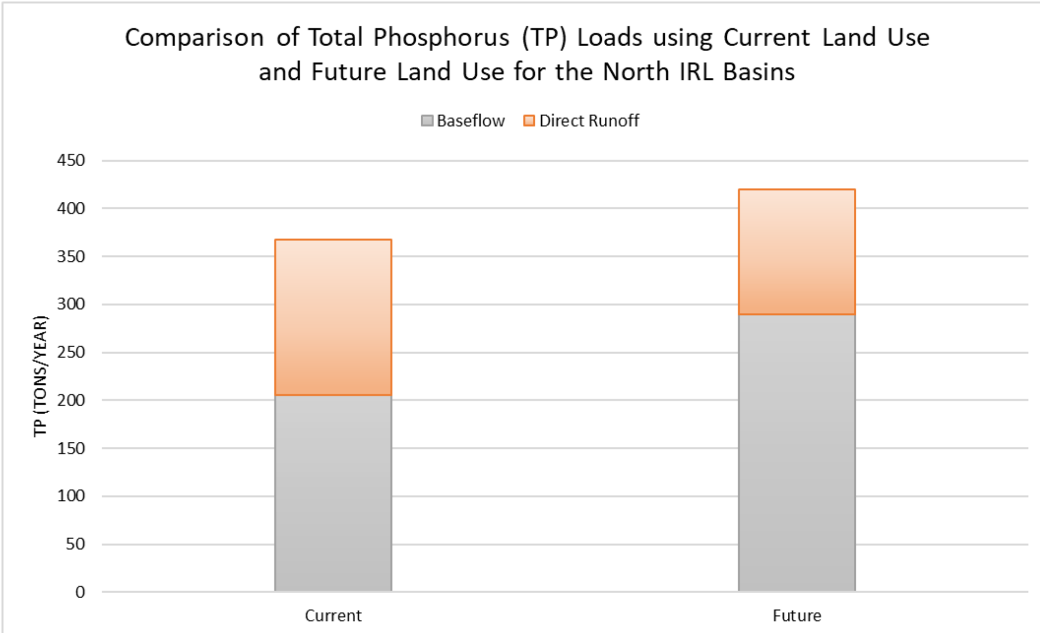


**Figure 23. Predicted baseflow and direct runoff TP loads within the NIRL watershed for both the current model year (2015) and future model year (2025).**

Figure 24, Figure 25, and Figure 26 present the predicted total volumes, TN, and TP loads for each basin of the modeled NIRL watershed for both the current year (2015) model run and the future year (2025) model run. Total volumes were predicted to increase across all basins, with the exception of IR1-3-A, which has specific baseflow conditions that resulted in a decrease of direct runoff; increases of over 20% were predicted in five basins. Estimated loads of both nutrients were predicted to increase across all basins, with an increase of over 20% in three basins for TN and four basins for TP. IRL1-3-B is predicted to have the greatest predicted increase in nutrient loadings from present to future conditions, with increases of 20.73 and 3.28 tons of TN and TP loads. Since rainfall was kept static between both model conditions (present and future), these increases are not rainfall driven, but simply driven by land use conversion changes. Other noticeable loading increases from present to future model conditions are visible at the IR5 basin, with increases of 16% for TN (16.3 tons) and 26% for TP (3.02 tons).

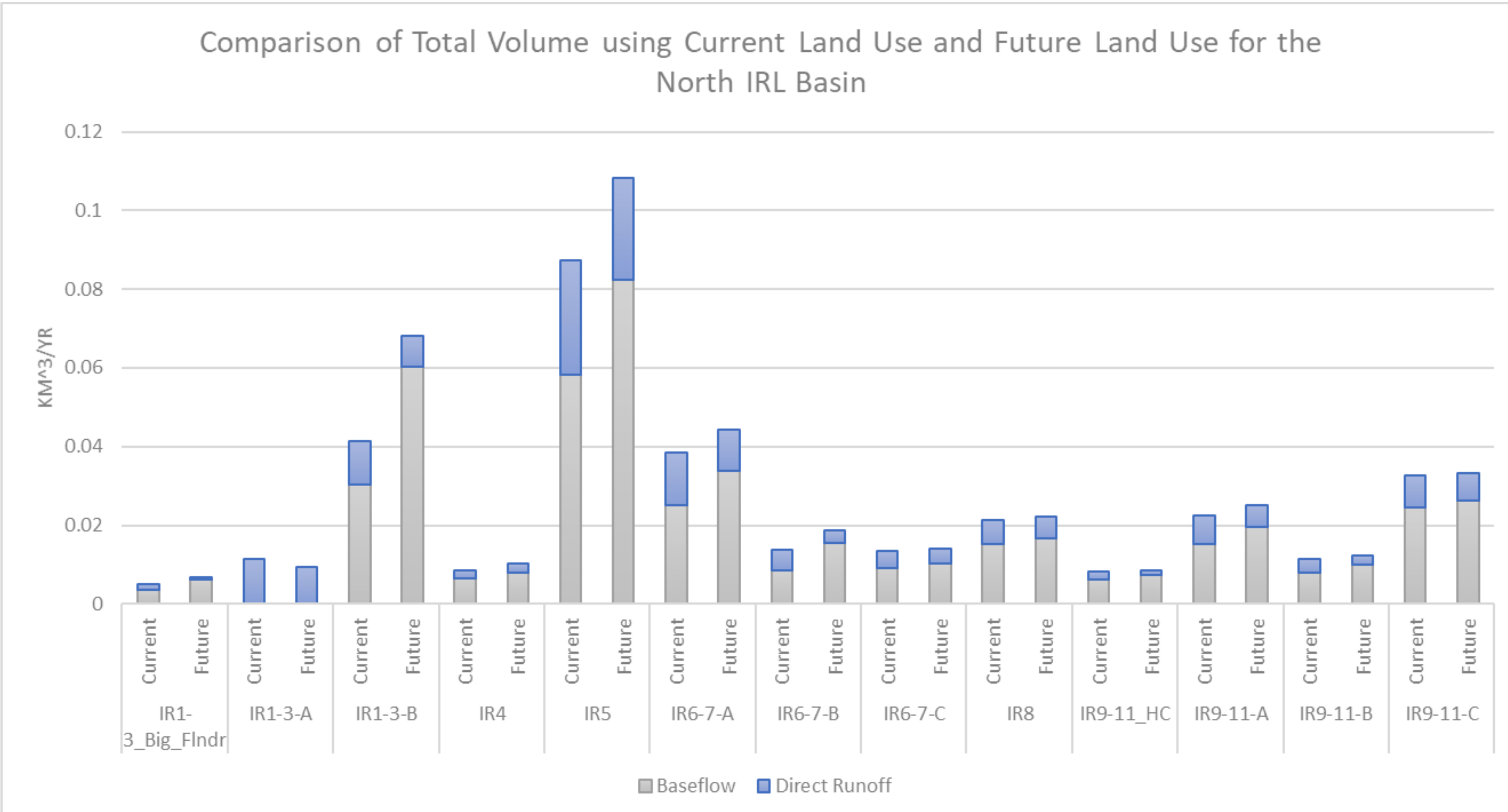


**Figure 24. Predicted baseflow and direct runoff total volumes for each basin of the NIRL watershed for both the current model year (2015) and future model year (2025).**

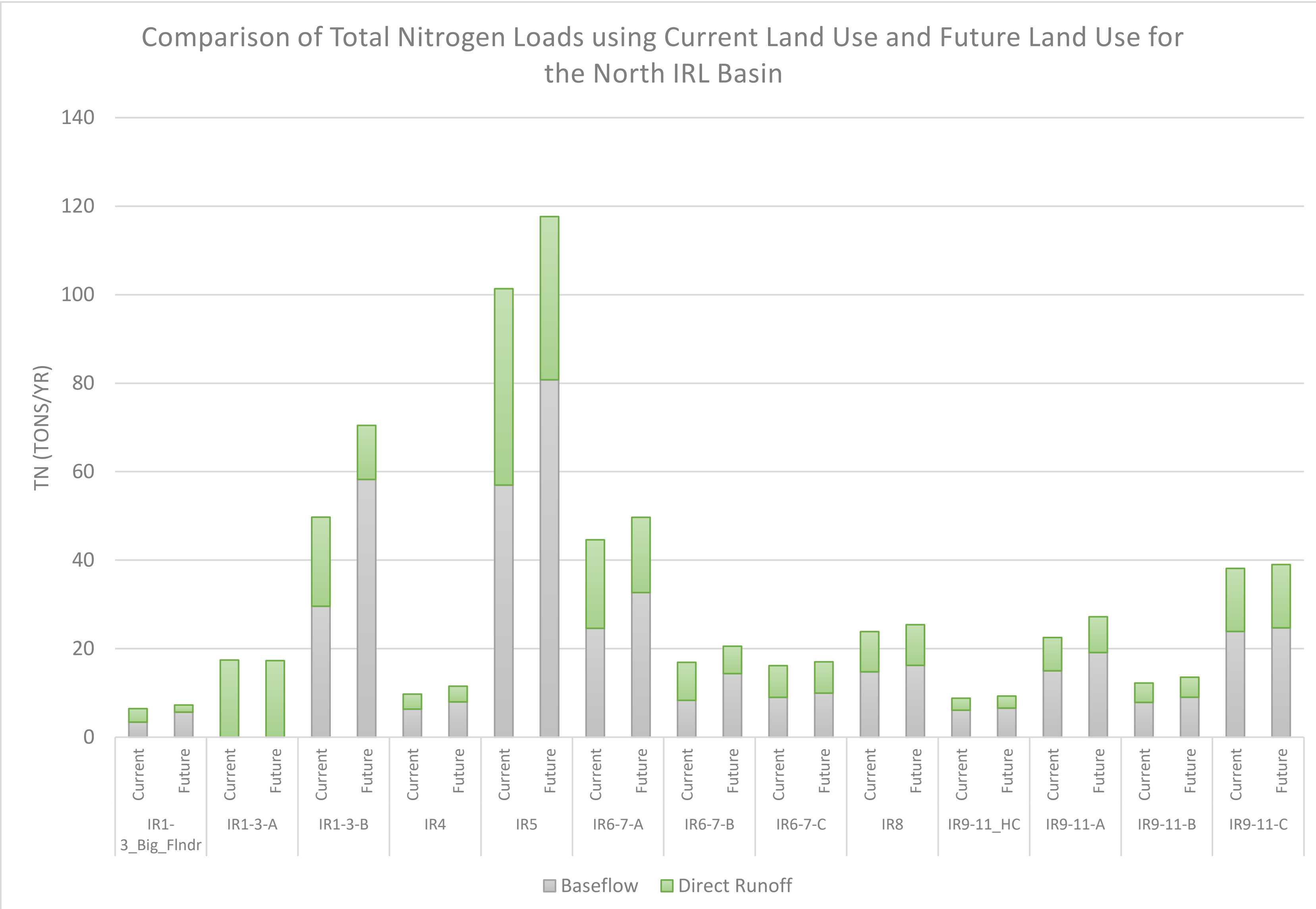


**Figure 25. Predicted baseflow and direct runoff TN loads for each basin of the NIRL watershed for both the current model year (2015) and future model year (2025).**

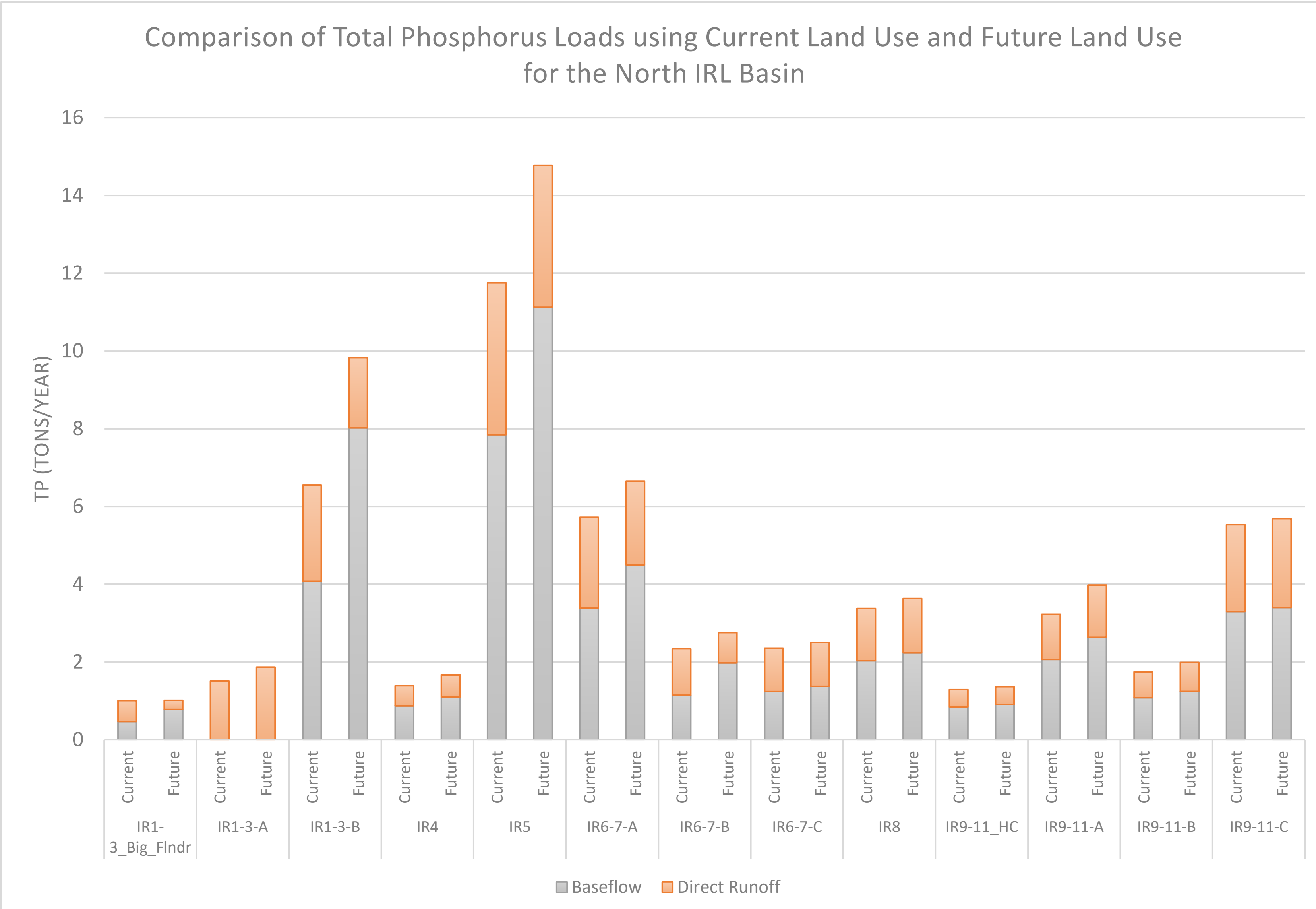


**Figure 26. Predicted baseflow and direct runoff TP loads for each basin of the NIRL watershed for both the current model year (2015) and future model year (2025).**

## Estimated Current Condition Baseloads for Military Bases (Aggregated SWIL Model)

Across the watersheds of both military bases, the distribution of total volumes is dominated by baseflow volumes, with PAFB having ca. 87% baseflow contributions while the volume contribution from CCAFS watershed is over 95% baseflow (99%) (Figure 27). These numbers were a direct result of measured flow and nutrient concentrations measured for both storm and baseflow conditions at both the PAFB and CCAFS. Baseflow contributions appear to be critical in these basins located with the Barrier Island of the Banana River Lagoon watershed.

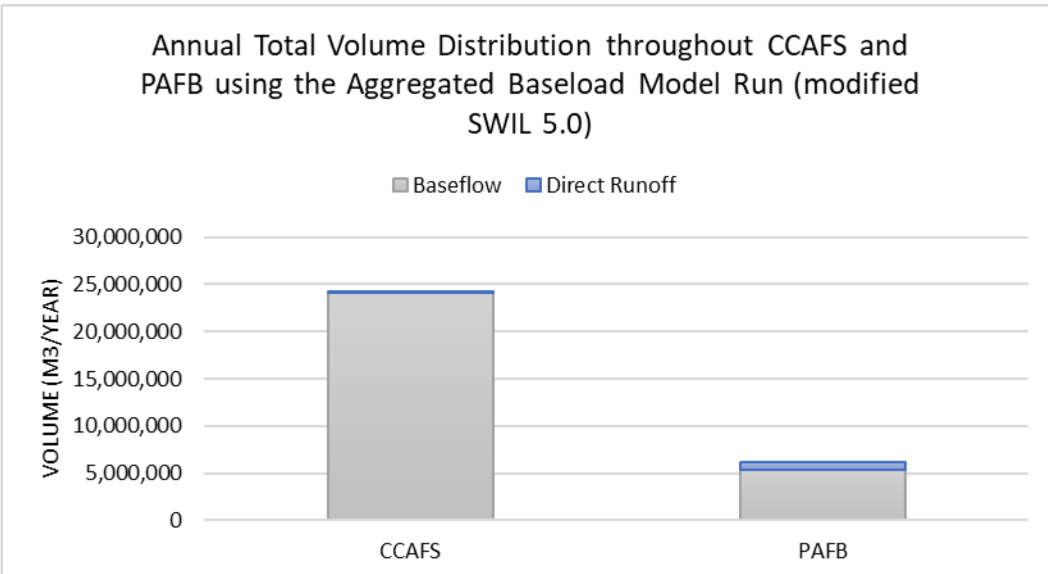


**Figure 27. Predicted baseflow and runoff volumes (in $m^3$) for CCAFS and PAFB using the Aggregated Baseload SWIL model.**

The pattern for the TN and TP loadings are very similar to the predicted volumes for the entire watershed, with TN having higher baseflow contributions than TP at both military bases (Figure 28 and Figure 29). The nutrient contribution of the CCAFS basins to the Banana River Lagoon is larger than those of the PAFB; this can be explained, in large part, to their relative size.

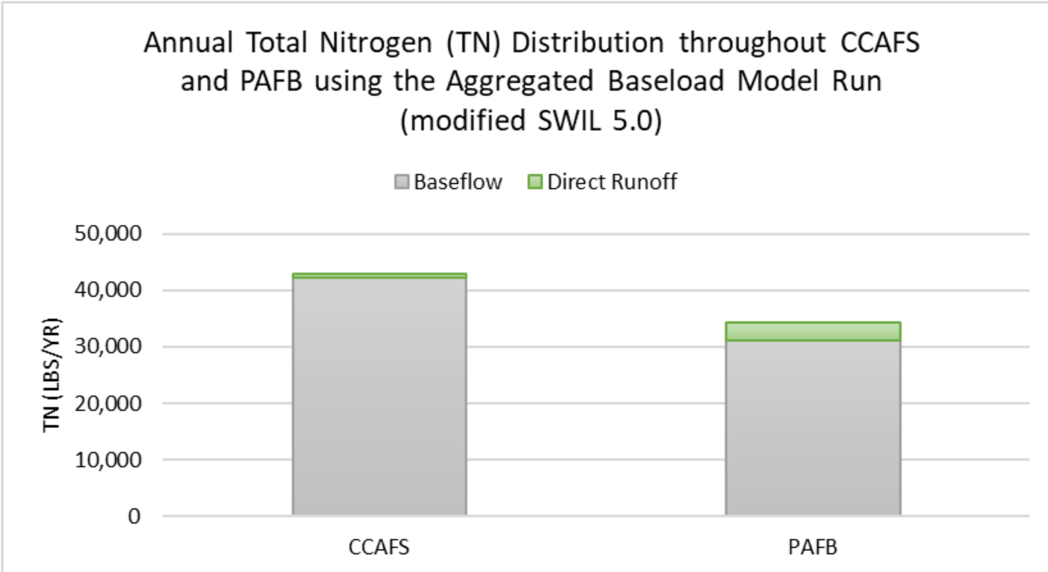


**Figure 28. Predicted baseflow and runoff loads of TN for CCAFS and PAFB using the Aggregated Baseload SWIL model.**

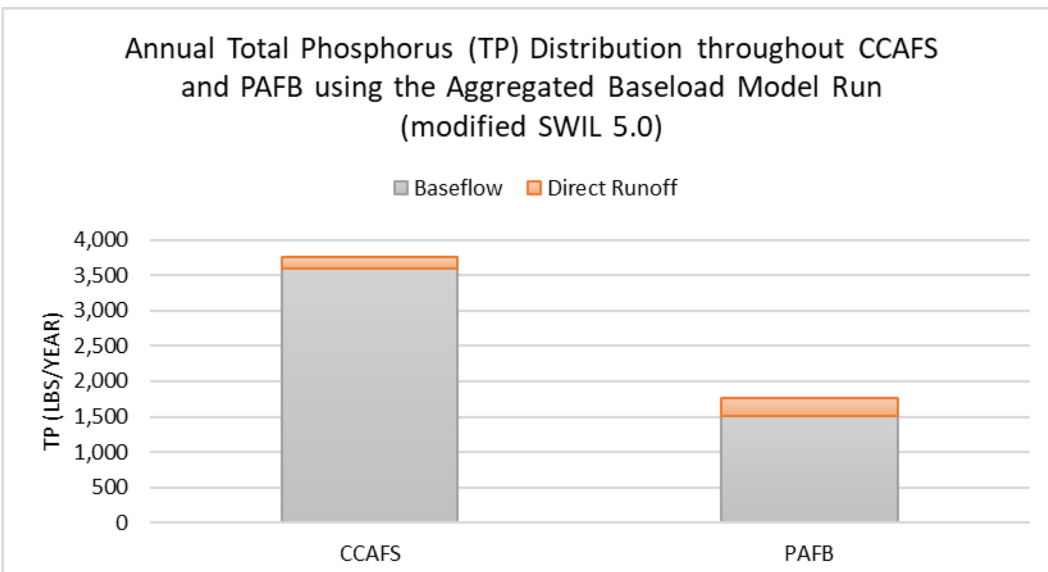


**Figure 29. Predicted baseflow and runoff loads of TP for CCAFS and PAFB using the Aggregated Baseload SWIL model.**

The spatial distribution of the predicted annual and seasonal loadings for TN and TP for each military base can be visualized in Figure 30 to Figure 35. For each of these predicted variables, the annual period of record (2004 – 2017) mean annual (January-December) and seasonal (January-May totals) were provided as "a" and "b" versions of the map. Higher loads appeared to be located within the CCAFS watershed, which is likely due to the larger overall area and soil type. As expected, the total volume, TN, and TP loading annual means are over three times higher than the dry seasonal mean corresponding values (January-May) for each military base (Figure 36 to Figure 38).

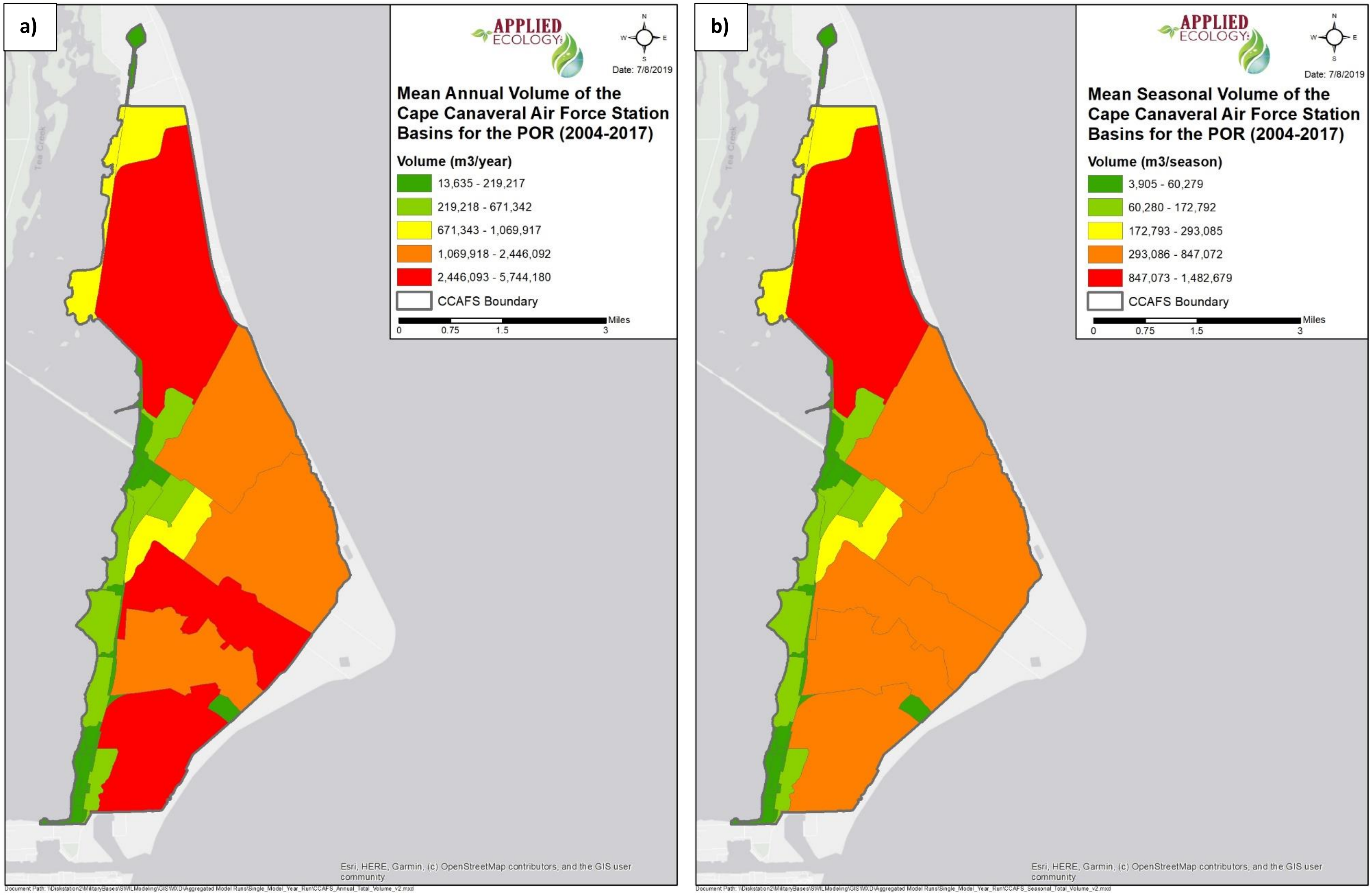


**Figure 30. Distribution of the (a) annual total volumes (m$^3$/year) and (b) seasonal total volumes (m$^3$/season) for each basin within the CCAFS TMDL boundary of the Aggregated Baseload model run.**

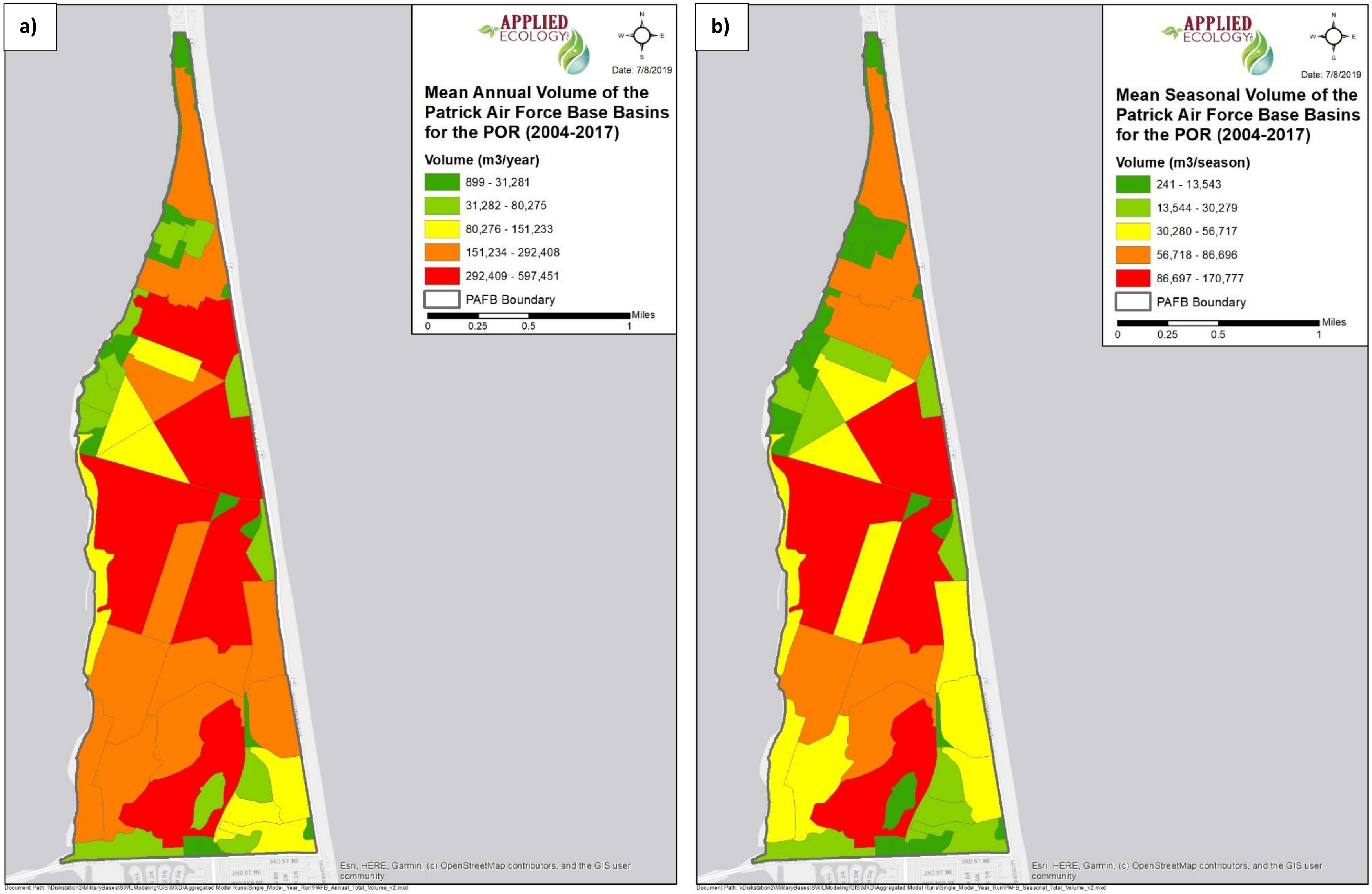


**Figure 31. Distribution of the (a) annual total volumes (m$^3$/year) and (b) seasonal total volumes (m$^3$/season) for each basin within the PAFB TMDL boundary of the Aggregated Baseload model run.**

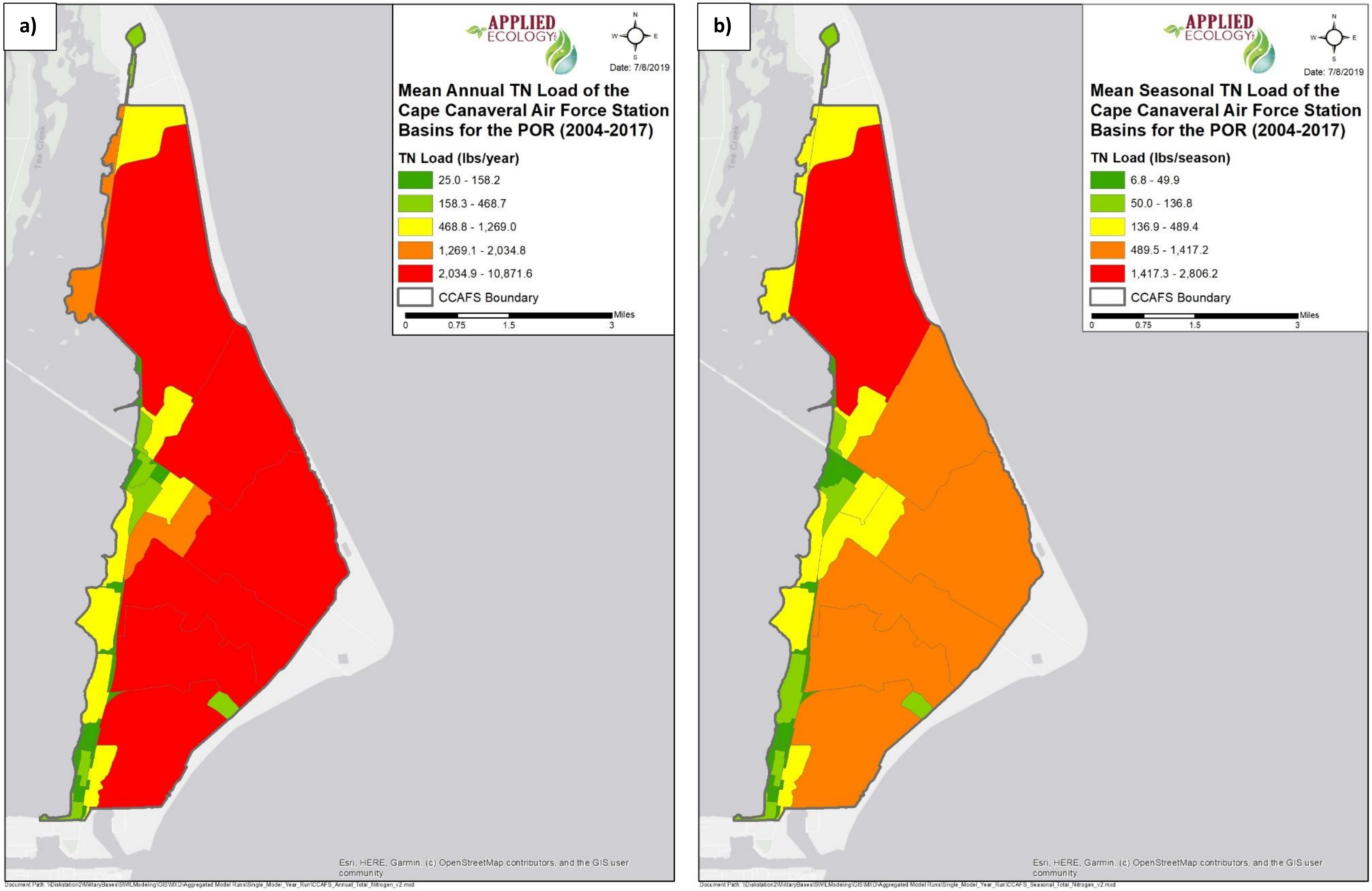


**Figure 32. Distribution of the (a) annual TN loads (lbs./year) and (b) seasonal TN loads (lbs./season) for each basin within the CCAFS TMDL boundary of the Aggregated Baseload model run.**

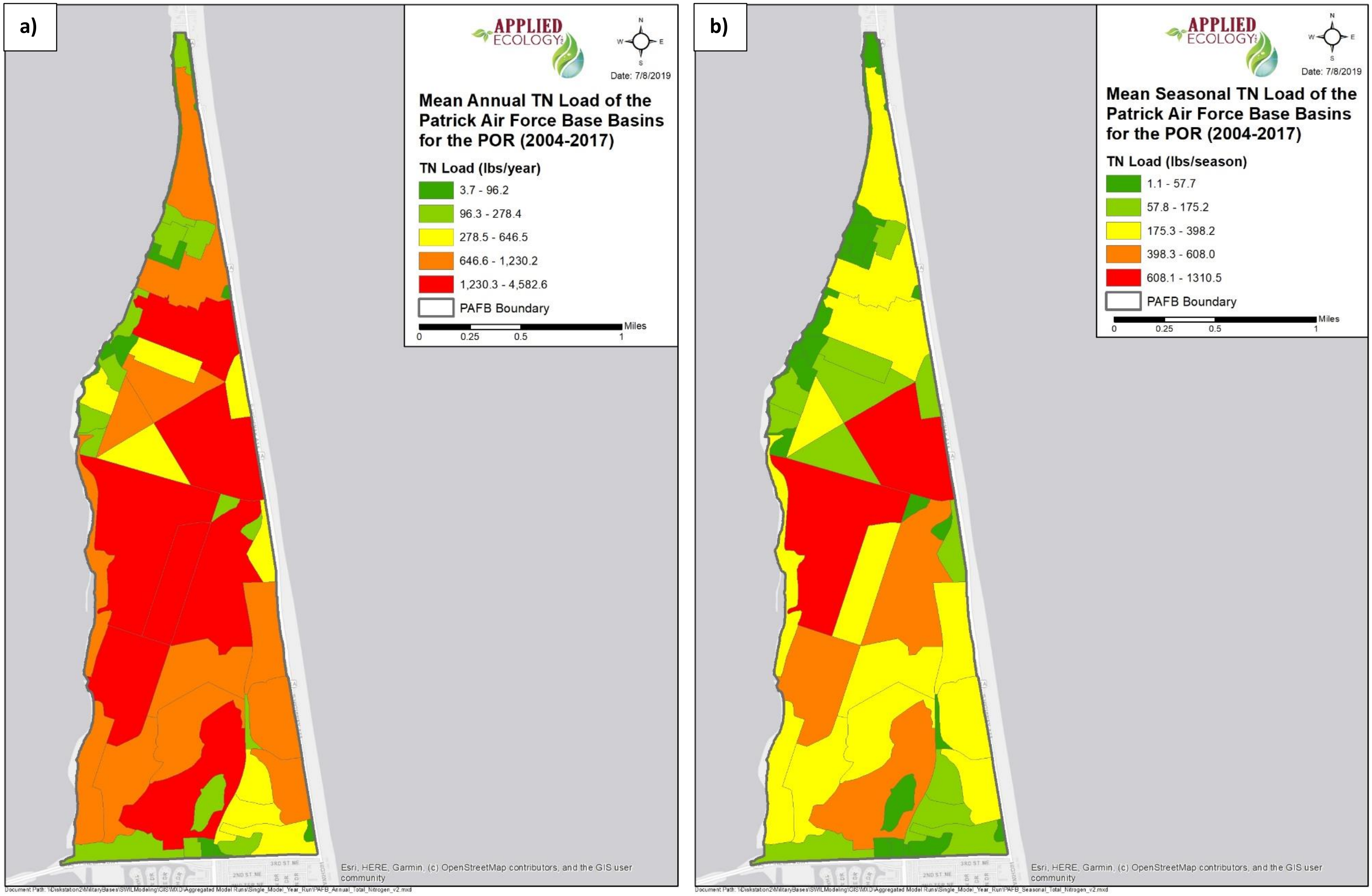


**Figure 33. Distribution of the (a) annual TN loads (lbs./year) and (b) seasonal TN loads (lbs./season) for each basin within the PAFB TMDL boundary of the Aggregated Baseload model run.**

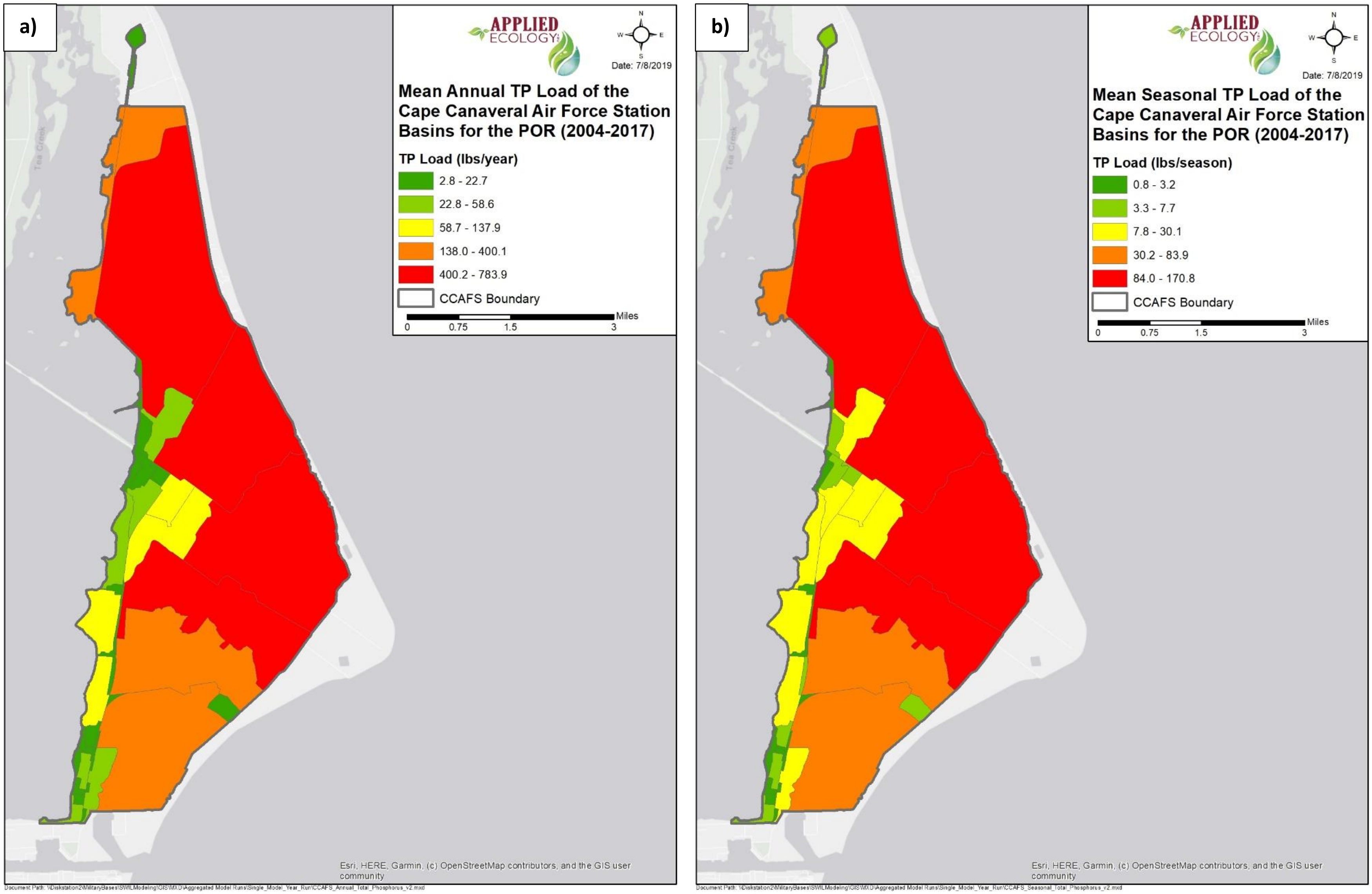


**Figure 34. Distribution of the (a) annual TP loads (lbs./year) and (b) seasonal TP loads (lbs./season) for each basin within the CCAFS TMDL boundary of the Aggregated Baseload model run.**

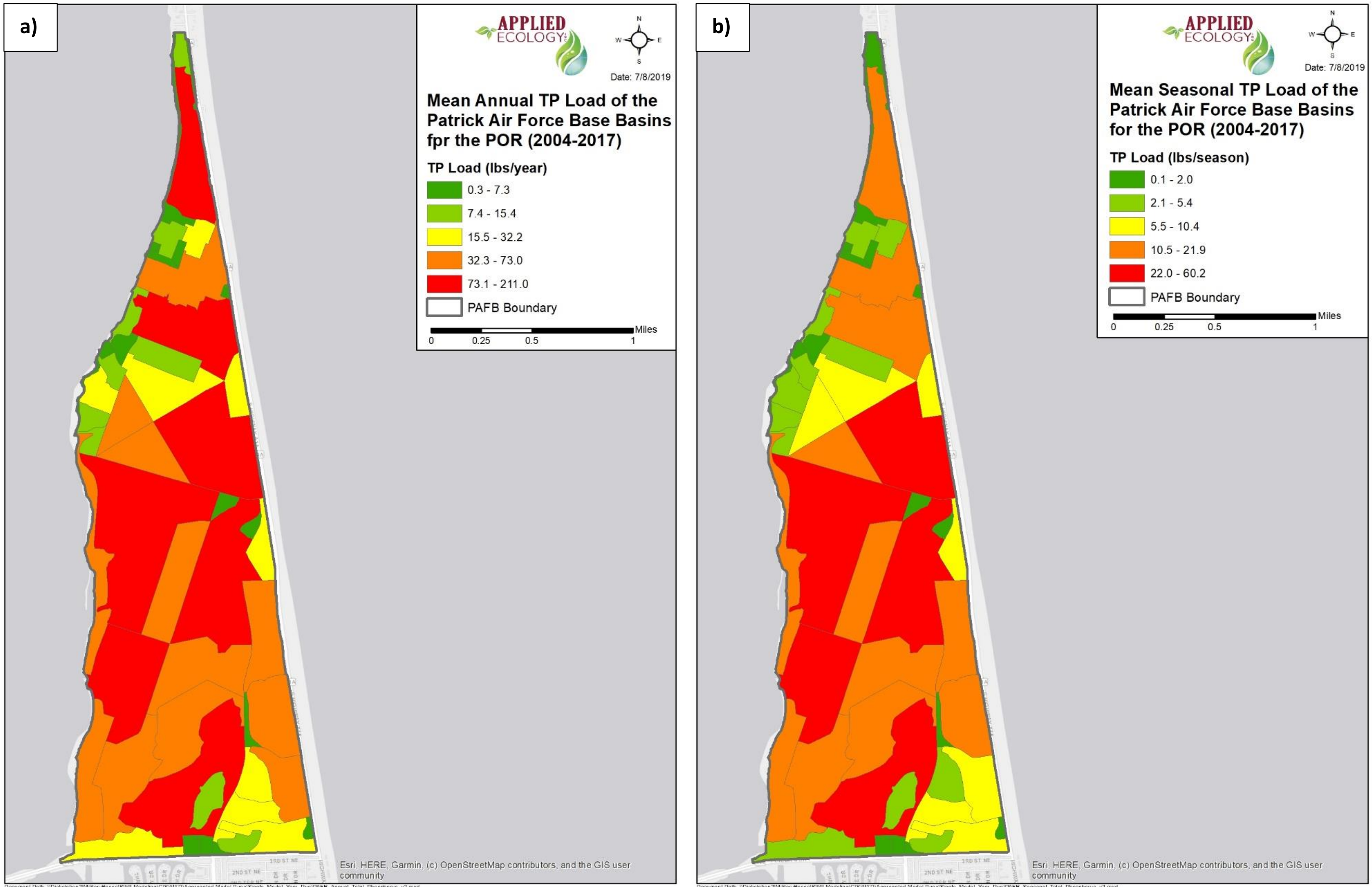


**Figure 35. Distribution of the (a) annual TP loads (lbs./year) and (b) seasonal TP loads (lbs./season) for each basin within the PAFB TMDL boundary of the Aggregated Baseload model run.**

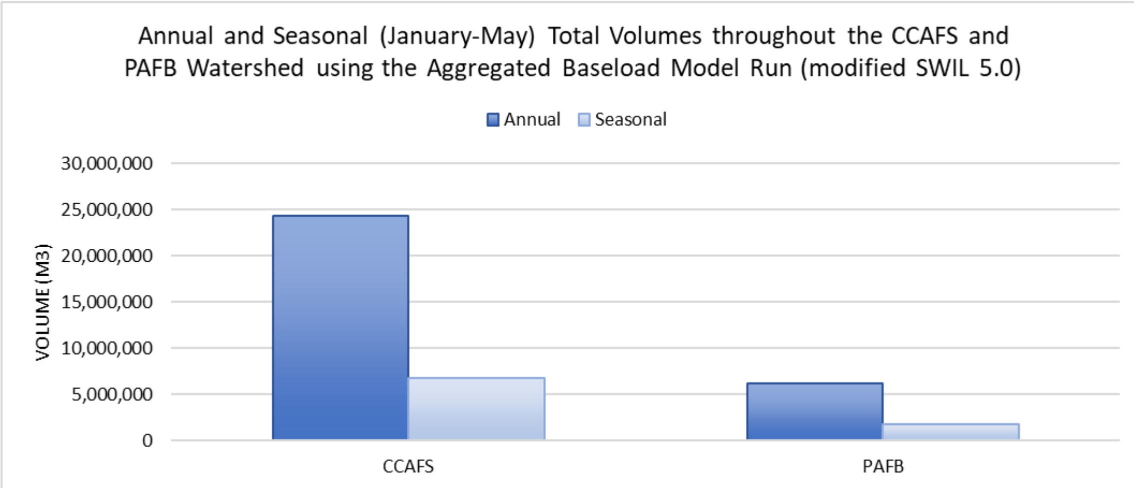


**Figure 36. Predicted annual and seasonal total volume distributions for the CCAFS and PAFB watersheds.**

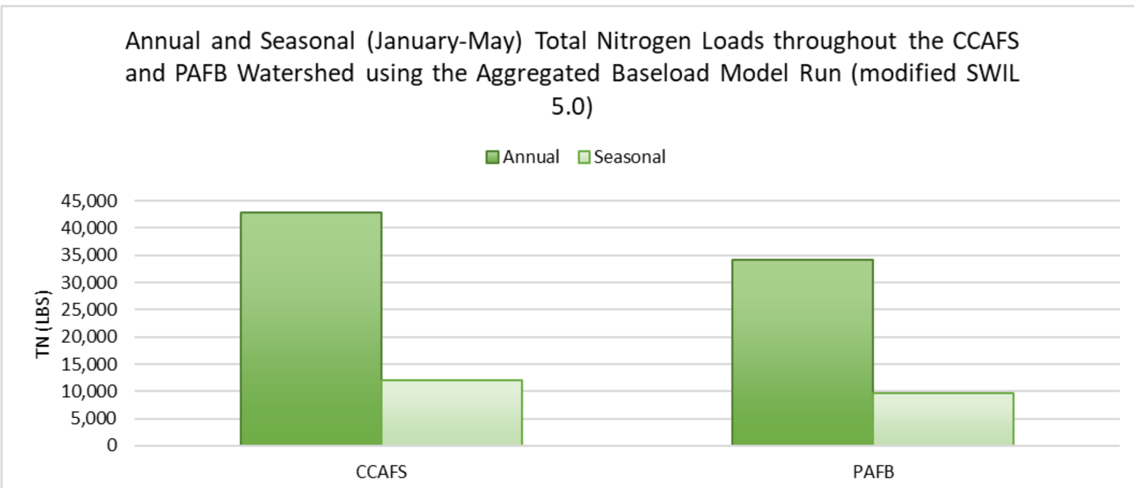


**Figure 37. Annual and seasonal TN load distributions for the CCAFS and PAFB watersheds.**

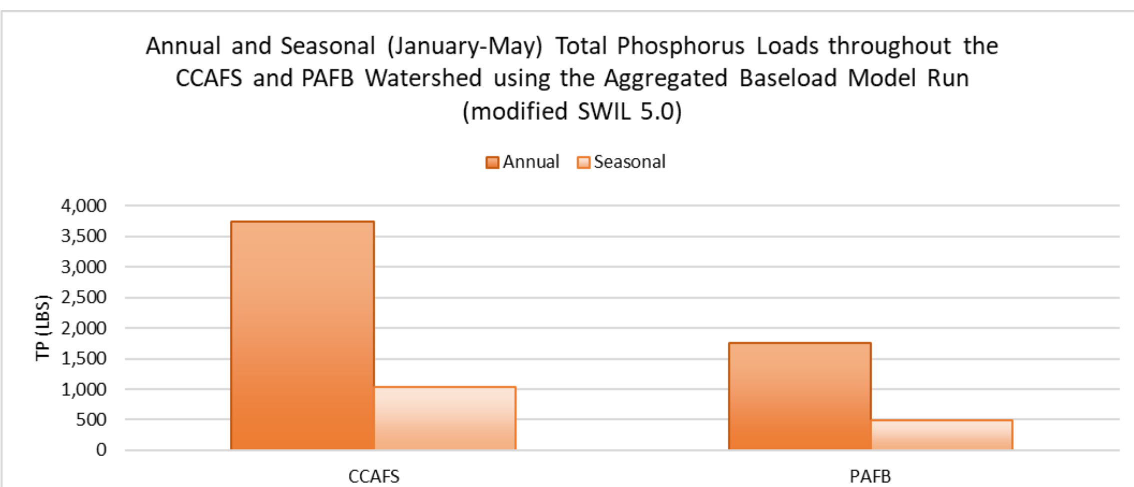


**Figure 38. Annual and seasonal TP load distributions for the CCAFS and PAFB watersheds.**

## Baseload Model Run Verification

### Cape Canaveral Air Force Station (CCAFS)

Overall, the Aggregated SWIL model version seems to slightly underestimate the total volumes and nutrient loadings. When comparing the outputs from the Aggregated SWIL model for CCAFS, an overall decrease of 6.8% was predicted for total volumes, TN, and TP (1,775,200 $m^3$/year, 3,139.6 lbs./year, and 275.0 lbs./year, respectively) (Figure 39); it is important to note that these decreases are almost entirely attributed to differences in baseflow rather than direct runoff. The total magnitude of the change between the two model versions is, however, negligible.

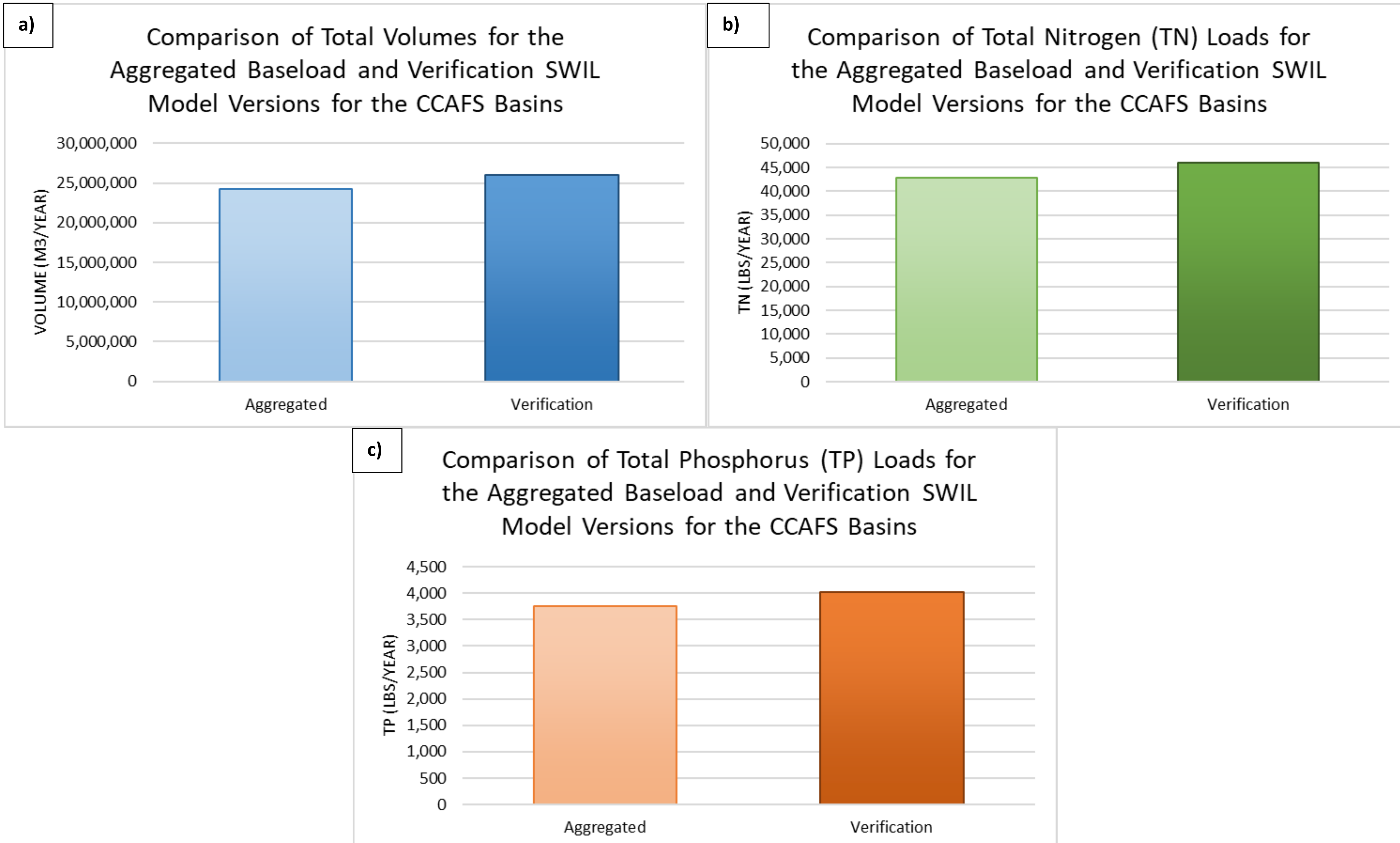


**Figure 39. (a) Total volume, (b) TN, and (c) TP outputs for the Aggregated Baseload and Verification SWIL model versions for the CCAFS.**

In terms of percent change, a majority of the individual basins experienced decreases which fell within the -10% and 5% class range for all three output types (Figure 40, Figure 41, and Figure 42). The largest decrease seen in any of the aforementioned classes for total volume was 39,421 $m^3$/year (Figure 40). There were some instances where decreases of ≥40% in total volume occurred; however, this only took place in one basin (basin 4A) and the magnitude of the decreases was negligible to the overall predicted volume output (never exceeded 3.5% of the total volumes for the Verification SWIL model for the months of interest).

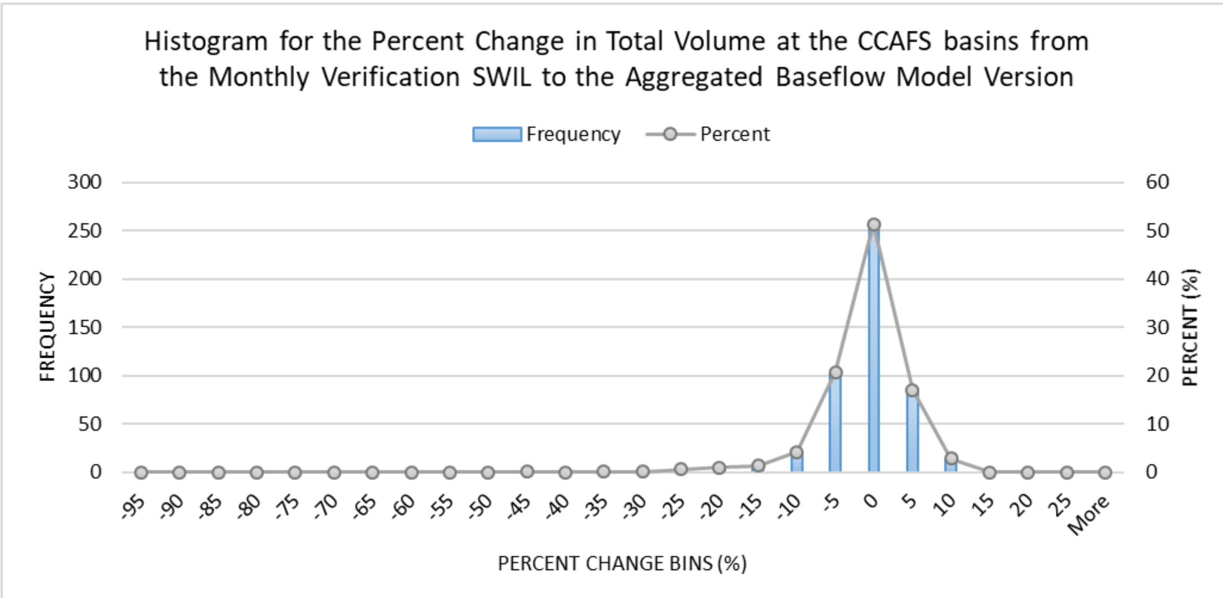


**Figure 40. Percent change histogram for total volumes of basins within the CCAFS watershed.**

The largest decreases seen in the -10% to 5% classes for TN and TP were 74.5 lbs./year and 6.4 lbs./year, respectively (Figure 41 and Figure 42). As with total volumes, one basin experienced a ≥40% decrease in nutrient loads, with the largest decreases of 72.4 lbs./year and 8.7 lbs./year, respectively. These are insignificant numbers when examining the overall nutrient loading from the entire CCAFS to the Banana River Lagoon.

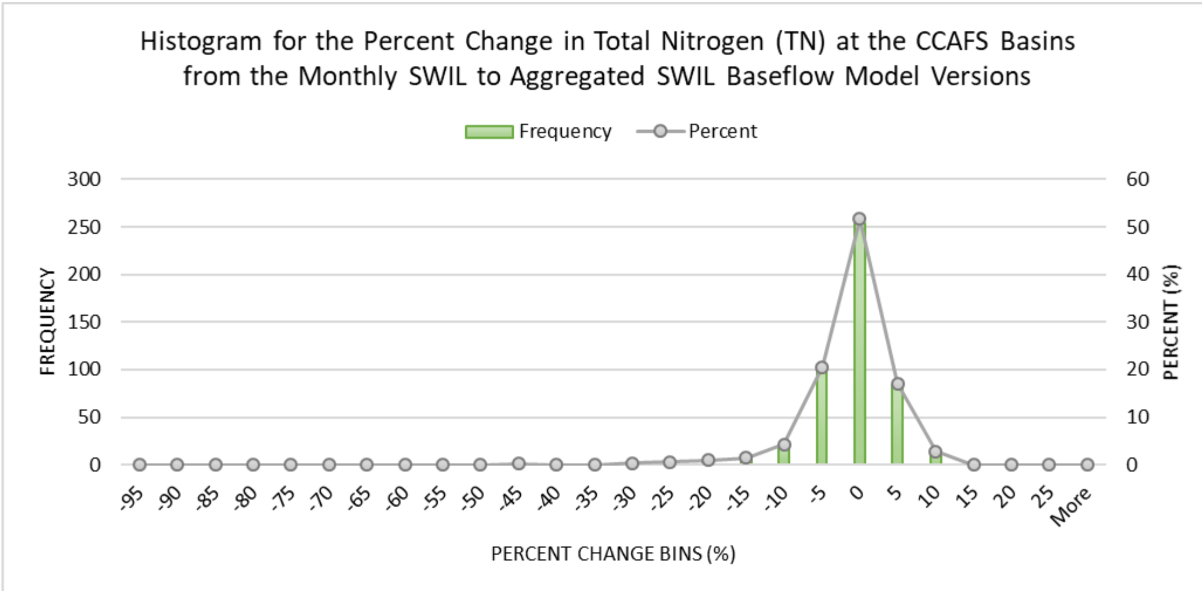


**Figure 41. Percent change histogram for TN for basins within the Group 1 verification subset.**

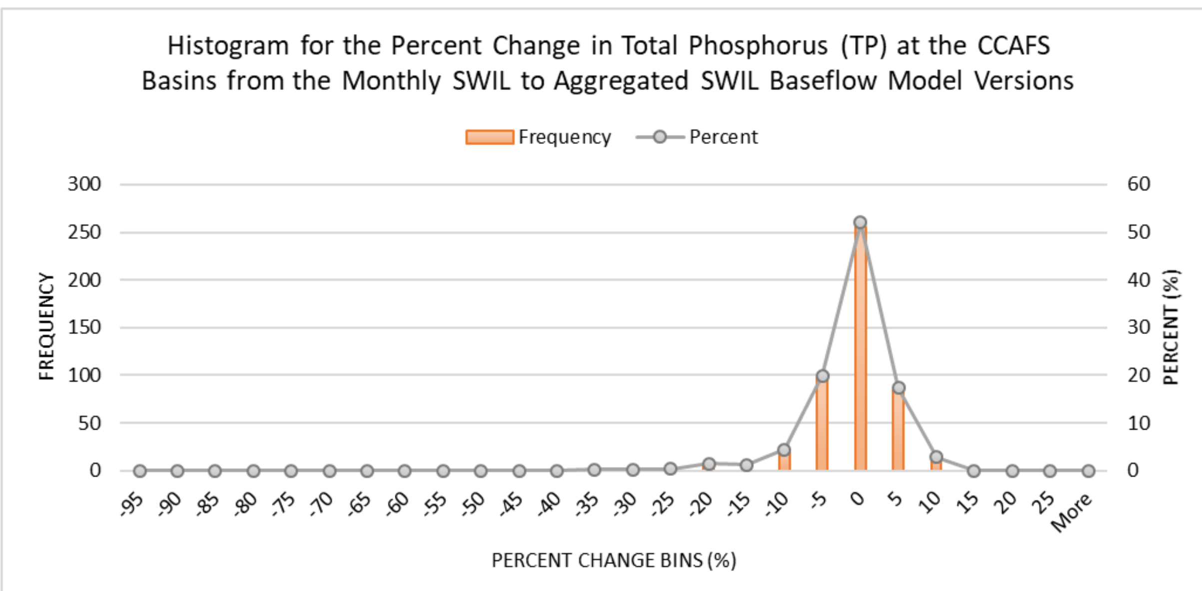


**Figure 42. Percent change histogram for TP of basins within the Group 1 verification subset.**

To further investigate if there were major discrepancies between the two model runs, linear regressions of the basin-specific outputs from both models were created for: 1) all months combined, 2) a representative dry season month (January), and 3) a representative wet season month (August). Comparison plots with respective regression coefficients ($R^2$) were created for volume, TN, and TP loading estimates (Figure 43). $R^2$ values were slightly lower for the dry season month than the wet season representative of all months combined, however, never below 0.99 for any regression. This clearly indicates that estimates from either the aggregated or monthly versions provide identical values for the basins within the CCAFS watershed.

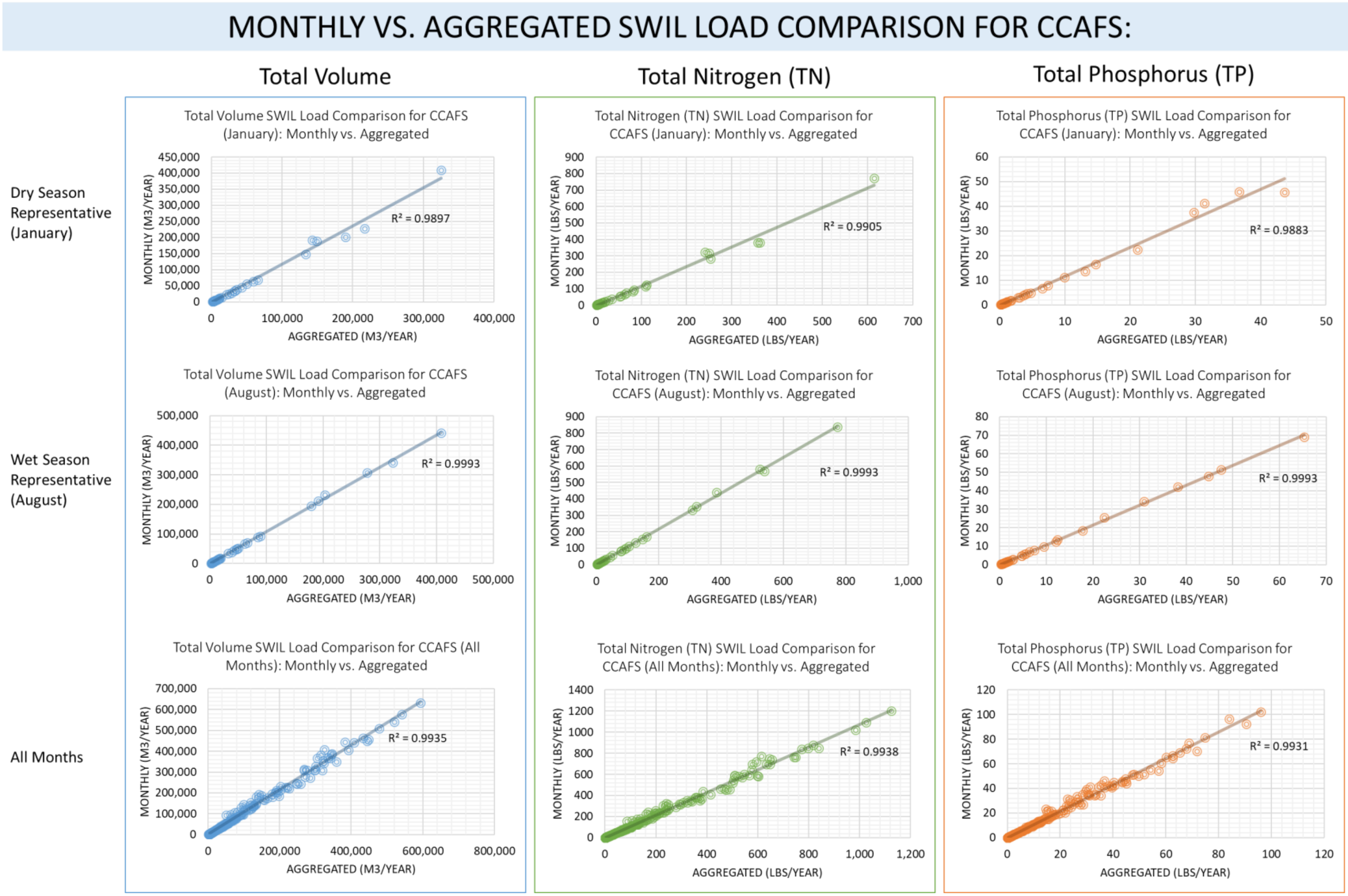


**Figure 43. Scatterplots and associated $R^2$ values for a representative dry season month (January), wet season month (August), and all individual months for total volume, TN, and TP for basins within the CCAFS watershed.**

## Patrick Air Force Base (PAFB)

As with the CCAFS, the aggregated model run seems to slightly underestimate the total volumes and nutrient loadings, although the decreases are negligible as the difference in total volumes were not greater than 1.1% (71,508 $m^3$/year). When comparing the nutrient outputs from the Aggregated to the Verification SWIL model for PAFB, overall decreases of 1.1% for TN and 1.0% for TP were predicted (371 lbs./year and 17.54 lbs./year, respectively) (Figure 44); it is important to note that these decreases are almost entirely attributed to difference in baseflow rather than direct runoff. The total magnitude of the change between the two model versions is, however, negligible.

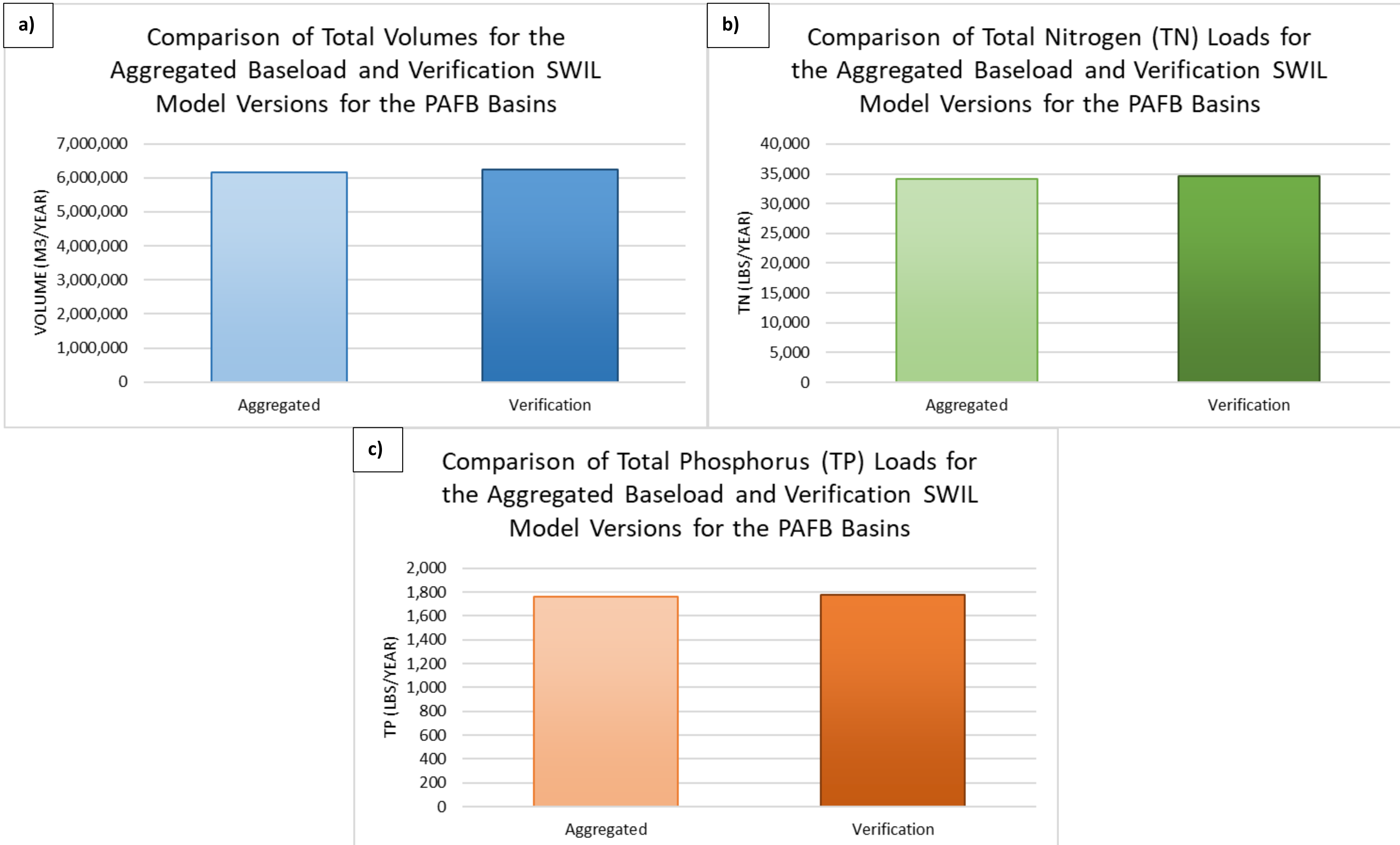


**Figure 44. (a) Total volume, (b) TN, and (c) TP outputs for the Aggregated Baseload and Verification SWIL model versions for the PAFB.**

In terms of percent change, a majority of the individual basins experienced decreases which fell within the -5% and 5% class range for all three output types (Figure 45, Figure 46, and Figure 47). The largest decrease seen in any of the aforementioned classes for total volume was 2,475 $m^3$/year (Figure 45). There was one instance where decreases of ≥15% in total volume occurred (basin 1G), however, the magnitude of the decreases was negligible to the overall predicted volume output (never exceeded 0.15% of the total volumes for the Verification SWIL model for that month).

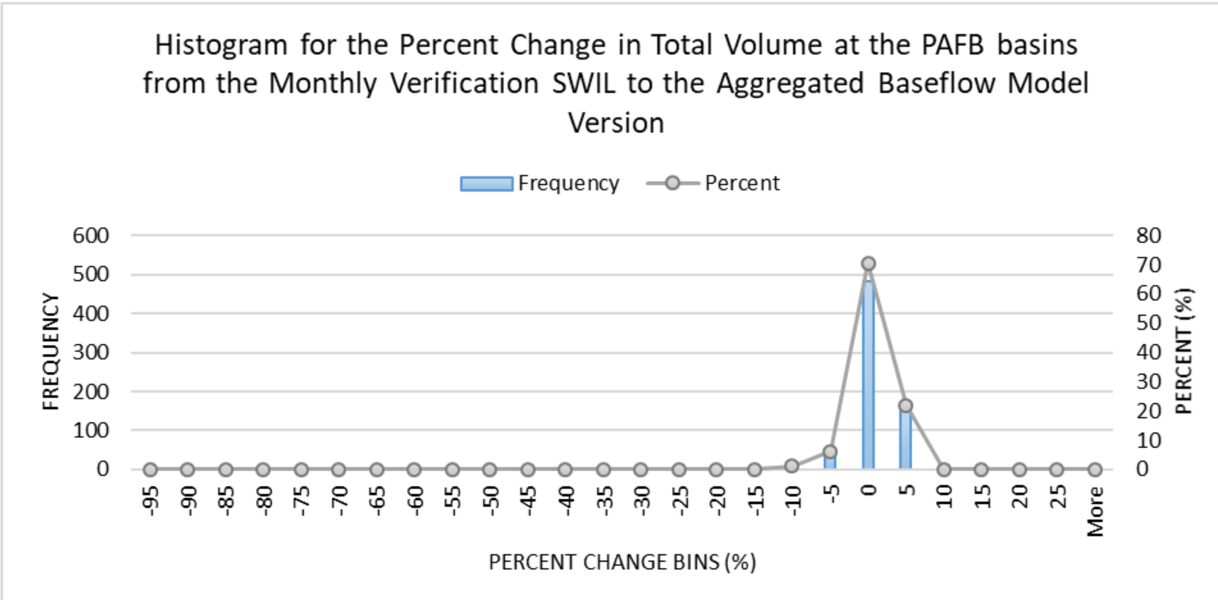


**Figure 45. Percent change histogram for total volumes of basins within the PAFB watershed.**

The largest decreases seen in the -5% to 5% classes for TN and TP were 19.0 lbs./year and 0.9 lbs./year, respectively (Figure 46 and Figure 47). As with total volumes, there was one basin (basin 1G) that experienced a few instances of ≥15% decrease in nutrient loads; however, the magnitude of the decreases was negligible (never exceeded 2.2 lbs./year for TN or 0.1 lbs./year for TP).

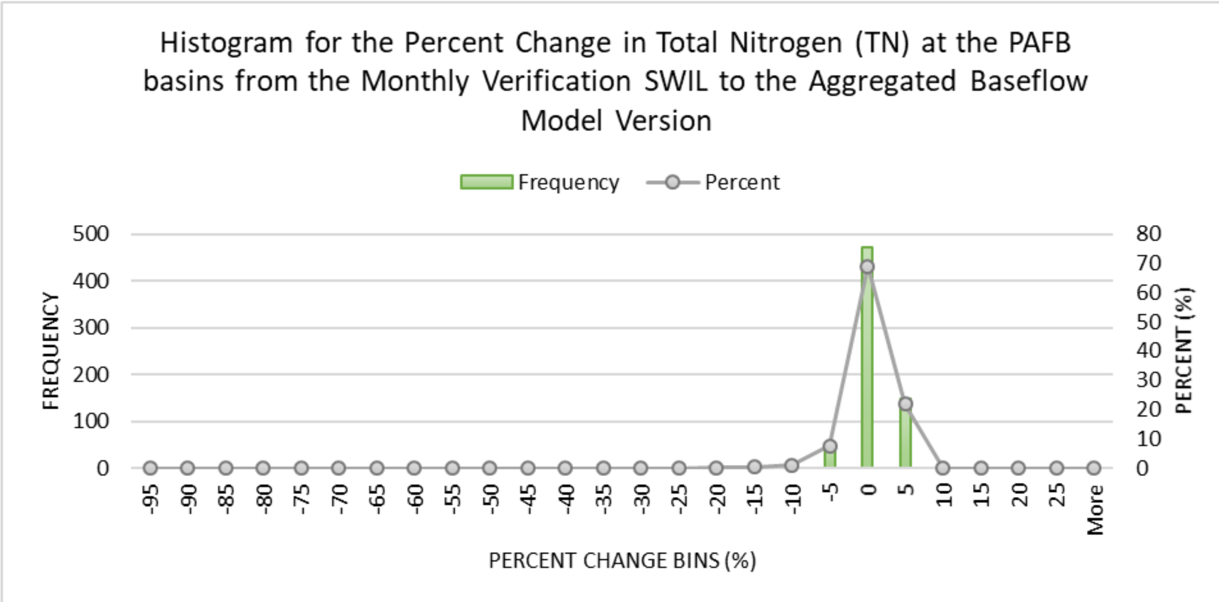


**Figure 46. Percent change histogram for TN for basins within the Group 1 verification subset.**

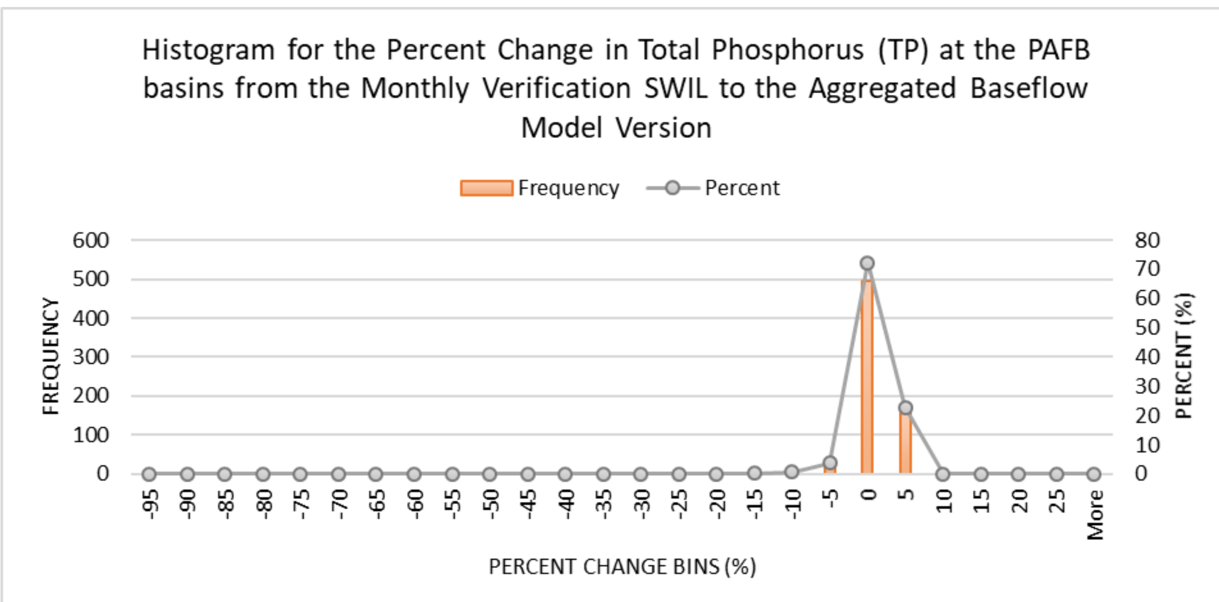


**Figure 47. Percent change histogram for TP of basins within the Group 1 verification subset.**

Once again, correlations between the outputs of both models were created in the form of regression scatterplots for total basin-specific volumes, TN, and TP loading estimates using: 1) all months combined, 2) a representative dry season month (January), and 3) a representative wet season month (August) to further investigate if there were major discrepancies between the two model runs (Figure 48). As with CCAFS, the $R^2$ values were slightly lower for the dry season month than the wet season representative of all months combined, however, never below 0.99 for any regression. This indicates both model versions do produce almost identical estimates for volumes and loads, and the overall pattern and data distribution for the PAFB watershed are extremely similar.

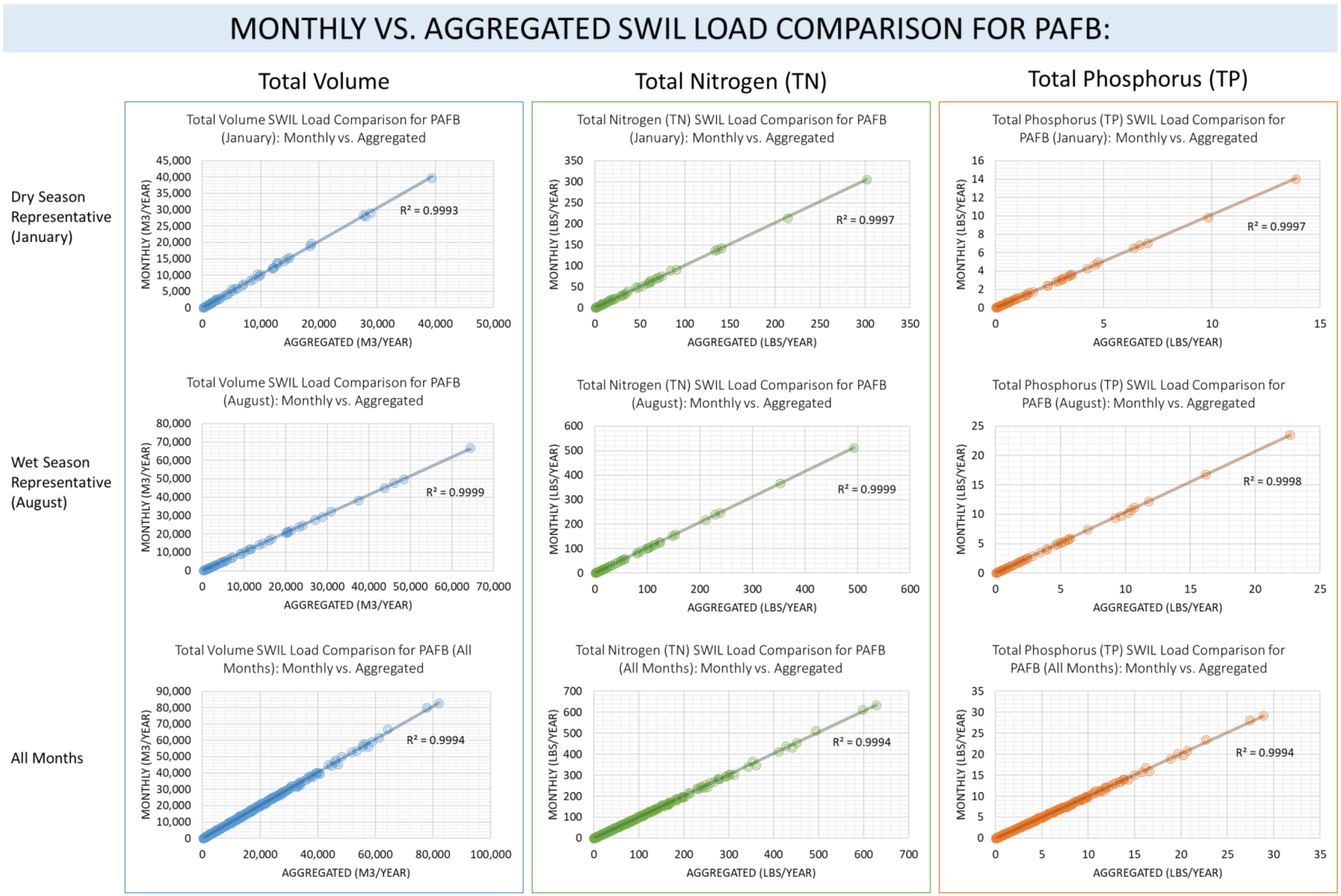


**Figure 48. Scatterplots and associated $R^2$ values for a representative dry season month (January), wet season month (August), and all individual months for total volume, TN, and TP for basins within the PAFB watershed.**

The verification efforts performed using randomized subsets covering large spatial extends of the model domain allow for the following conclusions:

- The aggregated model version (Aggregated Baseload SWIL) minimally underpredicts total volumes and loadings in comparison to the monthly model version (Verification SWIL)
- Magnitude of the differences between the two model versions, once aggregated to the entire subset basins, is insignificant or negligible at PAFB, with TN or TP underestimated values never exceeding 19.0 and 0.9 lbs., respectively
- Magnitude of the differences between the two model versions is slightly more substantial at CCAFS and are driven by a decrease in baseflow for the aggregated model outputs; however, with TN or TP underestimated values never exceed 158.4 and 12.4 lbs., respectively
- Spatial distribution of volumes and loading patterns is identical between the two model versions for the watersheds of both military bases, with correlation coefficients ($R^2$) consistently greater than 0.99

# Acknowledgements

Funding for this project was provided by the Florida State Legislature as part of the Florida Department of Environmental Protection Grant Agreement No. S0714 – Brevard County Muck Dredging. Special thanks to the members of the Florida Institute of Technology Indian River Lagoon Research Institute and Brevard County Natural Resources Management Department who provided valuable input and guidance throughout this project.

# References

Adkins, M., Mao, M., Taulor, M., Green, W., Basci, C., Bergman, M., and Smith, D. 2004. Watershed Model Development for the Indian River Lagoon Basin: Providing Simulated Runoff and Pollution Load to the Indian River Lagoon Pollution Load Reduction Model. Technical Memorandum 50, St. Johns River Water Management District, Palatka, Fla.

Bergman, M., and L. Donnangelo. 1995. Development of HSPF hydrologic simulation models for the Fellsmere Water Control District-East. Technical Memorandum 10, St. Johns River Water Management District, Palatka, Fla.

Bergman, M., and L. Donnangelo. 1996a. Development of HSPF hydrologic simulation models for the South Prong drainage basin of the Sebastian River. Technical Memorandum 15, St. Johns River Water Management District, Palatka, Fla.

Bergman, M., and L. Donnangelo. 1996b. Development of HSPF hydrologic simulation models for the North Prong drainage basin of the Sebastian River. Technical Memorandum 18, St. Johns River Water Management District, Palatka, Fla.

Bergman, M., and L. Donnangelo. 1998. Simulation of freshwater discharges to the Sebastian River using regional parameters. Technical Memorandum 25, St. Johns River Water Management District, Palatka, Fla.

Bergman, M., L. Donnangelo, and W. Green. 2001. Simulation of sediment, phosphorus, and nitrogen storm loads in the South Prong watershed of the Sebastian River, Florida, using HSPF/BASINS. Technical Memorandum 43, St. Johns River Water Management District, Palatka, Fla.

Gao, Xueqing. 2009. TMDL Report. Nutrient and Dissolved Oxygen TMDLs for the Indian River Lagoon and Banana River Lagoon. Florida Department of Environmental Protection.

Harper, H.H. and Baker, D.M. 2007. Evaluation of Current Stormwater Design Criteria within the State of Florida. Final Report submitted to the Florida Department of Environmental Protection for Agreement SO108 by Environmental Research & Design, Inc.

Harper, H.H. and Baker, D.M. 2015. Refining the Indian River Lagoon TMDL, Technical Memorandum Report: Assessment and Evaluation of Model Input Parameters. Final Report submitted to Brevard County Natural Resources by Environmental Research & Design, Inc.

Listopad, C. 2015. Spatial Watershed Iterative Loading (SWIL) Model Methodology Report; Updated for SWIL 3.0. Final Report submitted to Brevard County Natural Resources Management Office by Applied Ecology, Inc.

Listopad, C. 2019. The Development of Baseload Spatial Input Layers for the Indian River Lagoon Watershed; Based on the Spatial Watershed Iterative Loading (SWIL) Model 4.0. Final Memorandum Report submitted to Brevard County Natural Resources Management Office by Applied Ecology, Inc.

Mu, Q., Zhao, M., & Running, S.W. (2011). Improvements to a MODIS Global Terrestrial Evapotranspiration Algorithm. Remote Sensing of Environment, 115, 1781-1800. doi:10.1016/j.rse.2011.02.019